COMPUTER MODELLING STUDIES OF THE DIFFUSION OF LOW MOLECULAR WEIGHT CYCLIC PDMS OLIGOMER IN PDMS POLYMER

A thesis presented

by

THOMAS KUBAI

to

The Faculty of Sciences, Health and Agriculture in fulfilment of the requirements for the degree of Master of Science in the subject of Physics

University of Limpopo

Turfloop, Polokwane

January 2007

Supervisors: Prof. P.E Ngoepe

: Dr. L. Ackermann

Abstract

Molecular dynamics simulations have been carried out in order to examine the mechanism of diffusion of molecules in amorphous polymer matrix. PDMS model was folded in to a periodic cell, generated by rotational isomeric state (RIS) method at a prescribed temperature and density. Molecular dynamics was used to study transport properties of cyclic PDMS oligomers (hexa-methylcyclotrisiloxane (D3), octa-methylcyclotetrasiloxane (D4) and deca-methylcyclopentasiloxane (D5) using Dreiding and COMPASS force fields. Diffusion coefficients were calculated from the Einstein relation. Only D3 penetrant reached the long time limit from which the Einstein relation is satisfied. Analysis of displacement versus time for all the penetrants in PDMS matrix indicates that the penetrant motion is characterized by relatively long periods interspersed with fairly long and small jumps. Transport of solvent molecules occurs by jumps between individual sections of free volume (cavity/hole) through temporarily open channels.

Declaration

I declare that the dissertation hereby submitted to the University of Limpopo for the degree of Master of Science was composed by me and that the work contained therein is my own, except where explicitly stated otherwise in the text.

Thomas Kubai

Acknowledgments

Acknowledgements

I express my warmest gratitude to my supervisor Professor Phuti Ngoepe for introducing me to the interesting world of polymers, for guidance and endless optimism during these years. Also for critical reading of my thesis and for his valuable comments and inputs. I also thank him for understanding my time consuming in sports and otherwise.

My special thanks go to Dr. Lutz Ackermann for sharing his ideas with me and acting as a second reviewer of my thesis. I am grateful to the whole staff and students of Materials Modelling Center for providing me the most convenient and unforgettable moments at the working time and at the free time. Also I would like to thank the University of Limpopo (Turfloop Campus) for affording me the opportunity and the environment, in the form of Materials Modelling Center - the state of art centre, where all this work was done.

The financial support from National Research Foundation (NRF) and Eskom is gratefully acknowledged.

I am grateful to my brothers Gabriel, Charles, Joseph, Sam, my sister Shalate and my mother Shetsilele for all the sacrifices they made for me. Special thank to my son Thato and her mother Kgaogelo for giving me the love and courage to complete my MSc degree.

Table of contents

List of figures

List of tables

CHAPTER 1

INTRODUCTION

In this chapter emphasis will be on the historical background of insulators and the literature review on the diffusion in polymer materials

1.1 General introduction

One of the challenges facing the electric utility industry over the years is maintaining a cost-efficient and reliable network that will last for a long time. Perhaps the most critical components in this regard are the insulators, arresters and bushings. Electrical insulators are very important in the electrical power system such as sub-station and distribution and transmission lines. Traditionally high voltage insulation was dominated by ceramics insulators.

1.2 Historical background

High voltage outdoor insulation are exposed to a multitude of extreme mechanical, electrical and environmental (humidity, acidity, etc.) stresses. Early electrical insulation was made from glass and porcelain (ceramics material), and these have dominated the insulation market for many years. The performance of this type of insulator has been the subject of many research projects, and application principles are well established.

1.2.1 Porcelain insulator

Porcelain has been the dominant, exclusive technology on distribution and high voltage transmission line application since the development of high voltage electrical power lines at the beginning of the 20^{th} century. Porcelain technology kept pace with

increasing strength requirements (demand by higher voltage levels, span length and building of conductors) with continued development in porcelain composition and strength.

Annealed glass insulators were limited to low voltage application as they were not strong to meet the mechanical strength requirement for suspension insulators application. The development of annealed glass insulator by the process of toughening in the 1930'strenghtened them and by the end of World War II they were applied in high voltage insulation [1]. They quickly gained popularity in Europe and spread throughout the world. Their popularity was mainly due to the fact that

- they are lightweight as compared to porcelain insulators
- last for a long time because they don't age from micro crack propagation
- and they are easy to inspect, and safe to handle

1.2.2 Polymer insulators

The problem with ceramic insulators in high voltage outdoor insulation is that they are prone to very high surface leakage currents and flashovers when installed in polluted and humid environmental conditions, e.g. sea coast environment and near cement, fertilizer and chemical plants. They have a low strength-to-weight ratio and they are brittle in nature which makes them vulnerable to vandalism and can be easily damaged during transportation and installation. They are also easily wettable. These problems were solved by the introduction of high strength fiberglass composite insulators with elastomeric covering or polymer insulators. They were first introduced in the late 1950's with the production of the first polymer insulator called epoxy [2], but it suffered from severe tracking and erosion [3]. This caused a layback in polymer insulators being used in electric insulation. With the development of technology and

extensive research, better polymer insulators were produced. The popularity of this brand of polymer was so enormous that it brought about severe slump in porcelain and glass insulator usage which led to many ceramic producing plants closing or changing to polymer insulators production. The advantage of this type of insulators is that they have a high mechanical strength-to-weight ratio as compared to porcelain and glass insulators, and comparable or better withstand high voltage than porcelain or glass insulators and are easy to handle. Their hydrophobic properties make them well suited for outdoor insulation and they typically perform exceptionally well in extremely polluted environment [4]. They are also resistant to vandalism, damage resulting from installation due to their flexibility [5] and are well suited for contaminated environments [6, 7]. However with all the good things about polymers insulators, they possess some disadvantages also. Ageing seems to be a real problem with polymer insulators and they are easily degraded in inert inorganic materials under exposure to discharge and arcing. Under rain and fog conditions, the presence of water droplets intensifies the electrical field strength on the surface of a polymer insulator, as a consequence the surface corona discharge from water droplets accelerates the ageing of the shed material of a polymer insulator. Superficial chemical changes caused by weathering and dry band arcing [8], erosion and tracking, which may ultimately lead to failure of the insulators [9], difficult to evaluate service life, unknown reliability, and difficult to detect faulty insulators [10] are the main problems facing polymer insulators. To minimize or eliminate some of these disadvantages, a wide range of materials and formulations have been tested in the production of polymeric insulators

1.3 Literature review

While computers have increased the range of systems which are possible to study, the techniques available have also grown tremendously. The growth has lead to an increase in the importance of computer simulations. This means that the calculations, which were not possible few years ago, are now trivial to perform. Despite these developments, computational techniques such as energy minimization, Molecular Dynamics, Molecular Mechanics, Monte Carlo and electronic structure techniques are used to fill the informational gap between fundamental materials-science and industrial applications. The techniques can be applied to a wide variety of systems. Computational techniques can help to understand and design complex materials and offer an attractive approach in many fields where experimental data is rare and difficult to obtain. As a result, using the computational methods, alone or in combination with experiments, it is possible to model and predict structures, characterize bonding in solids, model surfaces and interfaces, atomic transport and defect structures, chemical reactions, phase transformations, docking or predict reaction mechanisms [11]

In this work molecular dynamics (MD) method is used to study the transport properties in amorphous polymer. It was first introduced by Alder and Wainwright in the late 1950's [12, 13] to study the interactions of hard spheres. It is one of the principal tools in the theoretical study of polymers. This computational method calculates the time dependent behavior of a molecular system. MD simulations microscopically provide detailed information on the fluctuations and conformational changes in polymer systems. The connection between microscopic simulations and macroscopic properties is made via statistical mechanics which provides the rigorous

mathematical expressions that relate macroscopic properties to the distribution and motion of the atoms and molecules of the N-body system; MD simulations provide the means to solve the equation of motion of the particles within the molecular system to get thermodynamic and time-dependent (kinetic) properties, eg diffusion.

Diffusion was studied before and it is generally accepted that the diffusion of small molecules in polymers occurs through a hop and jump mechanism. For relatively long periods of time (typically 100ps) penetrant stays in a certain small region of space. During this quasi-stationary period, the diffusion molecule is reflected by the walls of the cavity it resides in, in a short time typically (1-2ps). These quasi-stationary periods are interrupted by quick jumps from one cavity to another in a very short space of time. This behaviour (penetrant jumping from one cavity to another) is of special interest for the examination of diffusion processes. Gusev and Suter [14] tried to explain this jumps events by implemented Transition State Theory (TST) in a 3-dimensional free energy field. They assumed that over the residence time of the polymer/penetrant system in a sorption "state", the polymer atoms execute uncorrelated harmonic vibrations around their equilibrium positions in the minimum energy configuration of the penetrant free polymer matrix. These motions consist of small-amplitude vibrations of bond lengths and bond angles and librations of torsion angles but could not find any correlation [14-17] The jump event occurs when occasional fluctuations in the density of the polymer open a hole in a cage that is large enough for a diffusing molecule to permit a considerable displacement, giving rise to diffusion [18]. This jump event determines the real diffusion of penetrants [19] and is sensitive to penetrant size and temperature. The state of the polymer (crystal or amorphous) also has an effect on diffusion.

Amorphous polymers have a higher diffusion rate than crystalline polymers, as the probability of creating a diffusing channel (from which a molecule can move from one cavity to another) is high. This is as a result of high fluctuation of amorphous polymers. The effect of penetrant size is such that smaller penetrants tend to find large enough diffusing channel more often than large penetrants; hence more frequent jumps than large penetrants [20- 22]. However; Egbo De Bo et al [23] found the diffusion coefficient of C_2HCl_3 to be higher than that of C_7H_8 and CO_2 to be higher than that of C_2H_4 in PDMS. They concluded that penetrant geometry has an influence on diffusity in a polymer and that the molecular size effect is less pronounced in rubber polymers.

1.4 Choice of polymer material

Today, a great deal has been learnt about the comparative performance of various designs and constructions of these components under different operating conditions.

Polymers can be synthesized to exhibit electrical properties that can be controlled over a wide range from insulator to semiconductor or metal. The choice of a polymer material for a specific application is critical. The electrical, physical and chemical properties of the surface of the polymer insulator are critical to the reliable performance of the insulator throughout its life span. PDMS has shown to be the most suitable polymer in this regard.

1.5 PDMS based insulator

Properties of PDMS

Silicone rubber used in the area of high voltage insulation is mainly based on PDMS. It has distinctive chemical and physical properties which set it apart from glass and

porcelain and other materials used for other polymer insulators. It consists of a polymer and filler which are vulcanized to give the required solid shape. The polymer has a flexible backbone which consists of the alternate Si-O bond with the inert methyl groups on the Si atom. The methyl groups are projected outwards and are responsible for the hydrophobic properties of the polymer. This polymer is used in various applications, where its rheological and interface properties are desired. Some key bulk properties of PDMS arise from the high and flexible backbone around the O atom in the backbone (135-180^o) [24] with an energy minimization at 145^o [24] which makes it easy for $-Si(CH_3)_2-$ to rotate around the backbone. The ionic character of the siloxane bond backbone (43%) [25] explains the high stability [26] of PDMS against oxidation and thermal degradation. The O atom act as an electron drain which, in turn, increases the stability even in the Si-CH_3 bonds, and makes the methyl group slightly polarized [25, 27]. However as the siloxane bond is partly ionic it is also susceptible to electrophilic or nucleophilic attack. As the attached methyl group only posseses a Van der Waals attraction, the intermolecular forces become low. The low intermolecular forces, the high flexibility in the siloxane bond together with the large internal free volume are reflected in the low glass transition temperature, T_g being lower than 120^{o}C and high diffusivity. It is thermally stable over a wide range of temperature (-50 to 180^{o}C). This is because of the stable Si-O bond. Its elasticity makes it resistant to vandalism and less prone to damage caused by installation as compared to porcelain and glass

1.6 Rational for studying oil transport in PDMS

The diffusion of small molecules in polymer has been studied extensively and is of considerable practical concern. Knowledge of the diffusion rate is essential in

designing equipment for devolatilization, since the molecular diffusion of the volatile component is normally the rate –limiting step of the process. The drying of coatings is also limited by the ability of solvents to diffuse to the surface, and often physical properties of coatings are significantly influenced by the presence of even trace amounts of solvents [28].

Electricity plays an important role in our lives. Long lasting reliable and safe means of electric supply is a necessity. Introduction of polymeric insulators has proved to be a more reliable and safe way of transporting electricity than its counterparts. A worst scenario can be when an insulator breaks mechanically and drops a line. Insulators in neighbouring towers should be able to take the extra load and survive the mechanical impulse associated with the drop event, in order to minimize the maintenance cost. Reliable and long lasting insulators are needed. Polysiloxane have been industrially exploited for a long time and nowadays they play an important role in different applications because of their high thermal stability, low surface tension and outstanding dielectric properties [29-31]. Their low surface tension makes them hydrophobic which is exploited by the electrical insulation industry. PDMS insulators have proved to be some of the best when it comes to reliability. This is mainly due to their ability to recover hydrophobicity after losing it, which makes them to retain their virgin properties over a long time. The loss and recovery is a key issue also for silicone elastomers used in medical applications [32]. The hydrophobic recovery is perceived to be as a result of low molecular weight PDMS oligomers (silicone oils) migrating from the bulk to the surface of the material [33-35]. It is also able to transfer its hydrophobic properties to a polluted layer due to the diffusion of these oligomers. Hence the need to study oil transportation in PDMS.

1.7 Intentions of the study

Diffusion of low molecular weight PDMS oligomers through PDMS polymer matrix will be studied under Dreiding and COMPASS force fields, using the molecular dynamics technique, where:

- Diffusion of PDMS cyclic oligomer, D3, D4 and D5 with reference to the dependence on penetrant (solvent) size, temperature and force-field will be looked in to.
- The results obtained thereof, will be compared to experimental results and the available results obtained using computer simulation techniques.

1.8 Outline of the thesis

Chapter 1 presents a brief overview of electrical insulation and literature review.

Chapter 2 gives the theoretical models used in the description and prediction of the molecules transport through polymer matrix.

Chapter 3 introduces computer simulation techniques (and in particular molecular dynamics simulations) which are essential tools to obtain a more detailed picture of the structure.

Chapter 4 presents results and discussions of the simulation of the penetrant diffusion process in the polymer matrix. Twenty penetrants of D3, D4 and D5 are inserted in a periodic box with the polymer sample consisting of a chain of 200 monomers. This is followed by MD simulation for a period of 5 ns. From these simulations, the diffusion coefficients are calculated. All results will be discussed and compared to other simulations and experimental data.

Chapter 5 gives conclusions and some recommendations of the study.

CHAPTER 2

COMPUTATIONAL METHODOLOGY

In this chapter emphasis will be on the method used in simulation of our system.

There are many approaches of computational chemistry which are popular in molecular modelling:

2.1 Simple comparative and graphical approaches - graphical inspection, molecular superposition, overlapping/nonoverlapping volume, topological indices, traditional SAR and QSAR, rigid conformational search, ComFA, shape analysis, etc. Used as a first step in scanning biologically active molecules and useful in detecting characteristic molecular features needed for activity. These methods are not quantitative, since they do not consider energetics of receptor-ligand interactions.

2.2 Quantum approaches - based on explicit consideration of the electronic structure. These methods are substantially more computationally demanding than comparative and empirical approaches for the molecules of the same size. They can be roughly divided into:

2.2.1 Semi-empirical methods - approximate methods in which some quantities are taken from experiment, some small quantities are neglected, and some quantities estimated by fitting to experimental data. May only be used for chemical species for which they were parameterized. For distorted, uncommon bonding situations produce unreliable results.

2.2.2 Non-empirical methods - do not require empirical parameters and can be used for any molecular system.

Traditional ab initio - use Hartree-Fock method as a starting point, i.e., wave function is used to describe electronic structure.

Density Functional Methods - electron density as a primary way of describing the system.

2.3. Empirical approaches - molecular mechanics, molecular dynamics. Relatively simple interatomic potentials, electrostatic interactions, and dispersion forces, allow for basic comparisons of energetics and geometry optimization. Solvent effects can be included explicitly or via empirical models. Very useful and fast compared to rigorous quantum calculations. Major drawbacks: experimental or theoretically derived information is needed to ``standardize" models and parameters. In principle, these approaches are not able to model chemical reactions, bond forming/breaking since electronic structure does not enter these models. This is the method that we are using in our simulation as it can handle large systems. Emphasis will be on molecular dynamics to predict the diffusion coefficients of small molecules in polymer matrix.

2.4 Molecular dynamics

2.4.1 Classical mechanics

Molecular dynamics is a useful tool in studying computationally the motion of individual atoms or molecules in a polymer. Molecular dynamics uses Newton's equation to simulate atomic motion

$$F_i = m_i a_i \qquad (1)$$

where F_i is the total force experienced by an atom, m is the mass of atom and a is the acceleration. Given a potential function $V(\bar{r})$ which depends on the position of all atoms, equation (1) can be written as

$$m_i \frac{d^2 \bar{r}_i}{dt^2} = -\nabla_i V(\bar{r}) \qquad (2)$$

where $\bar{r}$ is the cartesian coordinates, t is the time and m is the mass of atom i. The potential energy $V(\bar{r})$ describes the Born-Oppenheimer surface for atomic motion. In practice the equations of motion cannot be solved exactly and have to be evaluated by use of finite difference methods. The simplest and most frequently used method, first used by Verlet, is obtained from the Taylor expansion of the coordinates $\bar{r}_i$ at times $t + \Delta t$ and $t - \Delta t$ about $r_i(t)$

$$\bar{r}_i(t \pm \Delta t) = \bar{r}_i(t) \pm \Delta t \frac{d\bar{r}_i(t)}{dt} + \frac{\Delta t^2 d^2 \bar{r}_i(t)}{2! dt^2} + \frac{\Delta t^3 d^3 \bar{r}_i(t)}{3! dt^3} + 0(\Delta t^4) \qquad (3)$$

adding the two expansions lead to the prediction of the position at time $t + \Delta t$

$$\bar{r}_i(t + \Delta t) \cong -r_i(t - \Delta t) + 2r_i(t) + \frac{\Delta t^2}{m_i} F_i(t) \qquad (4)$$

the velocities do not appear in this equation but are useful in the calculation of kinetic energy and hence the total energy. They can be evaluated from the position by:-

$$v(t) = \frac{\{r_i(t + \Delta t) - r_i(t - \Delta t)\}}{2\Delta t} \tag{5}$$

Another integration algorithm in which the velocity is incorporated, is the leap-frog algorithm. This is essentially equal to the Verlet algorithm and is given by two steps:-

$$v_i(t + \frac{\Delta t}{2}) = v_i(t - \frac{\Delta t}{2}) + \frac{\Delta t}{m_i} F_i \tag{6a}$$

$$r_i(t + \Delta t) = r_i(t) + \Delta t v_i(t + \frac{\Delta t}{2}) \tag{6b}$$

where Δt denotes the time step and F_i is the total force acting on the atom. By specifying position and velocities of the particle as a function of time, trajectories can be processed to extract static and dynamic properties of interest.

2.4.2 Molecular mechanics

Molecular mechanics is a method which represents molecules as spheres connected by springs, observable data is used to parameterize constants based on Hooke's Law, allowing systems to be represented by Classical physics and simple potential energy functions. This method ignores the explicit presence of electrons which enables larger systems to be calculated but the drawback of this method is that it is only useful the description of molecular ground states, making it difficult to follow reaction paths. It is a relatively cheap calculation although the accuracy of the calculation is highly

dependant on the system used to parameterize the constant and its similarity to the system under study.

2.5 The potential energy surface

The complete mathematical description of a molecule, including both quantum mechanical and relativistic effects, is a formidable problem, due to the small scales and large velocities. Since no complete relativistic quantum mechanical theory is suitable for the description of molecules, this discussion starts with the nonrelativistic, time-independent form of the Schrödinger description:

$$H\psi(R,r) = E\psi(R,r) \tag{7}$$

where H is the Hamiltonian for the system, ψ is the wave function, and E is the energy. In general, ψ is a function of the coordinates of the nuclei (R) and of the electrons (r).

The Born-Oppenheimer approximation

If equation (7) is solved for the total wave function ψ then everything about the system will be known. But it is too complex for any practical use, so approximations are made. Since the mass of the electrons is very small as compared to that of the nuclei, and they (electron) move much faster, Born and Oppenheimer proposed what is known as the Born-Oppenheimer approximation: the motion of the electrons can be decoupled from that of the nuclei, giving two separate equations.

$$H_e\phi_e(r,R) = E_e\phi_e(r,R) \tag{8}$$

Where ϕ is the electronic wavefunction and it depends upon the nuclear position R. This equation defines the potential energy surface $E(R)$ as a function of the coordinates of the nuclei.

$$H_N\phi_N(R) = E_{tot}\phi_N(R) \tag{9}$$

Equation (9) then describes the motion of the nuclei on this potential energy surface $E(R)$. Solving equation (9) is important if you a re interested in the structure or time evolution of a model. In principle equation (8) could be solved for the potential energy E, and then equation (9) can be solved. However the effort required solving equation 8 is very, large, so usually an empirical fit to the potential energy surface, commonly known as force field is used.

2.6 Force fields

The basis of all molecular simulation methods is a potential energy function $V(\bar{r})$. This function gives the potential energy of a system containing N atoms and depends on the position $\bar{r}_i$ of each atom. Ideally one would like to obtain this energy quantum chemically in which case $V(\bar{r})$ would describe the Born-Oppenheimer surface for the motion of the nuclei. In practice this would only be feasible for systems containing a few atoms whose dynamics could then only be simulated for very short time due to the large computational time spent to evaluate $V(\bar{r})$ throughout the simulation. With the advance of computer hardware, and the introduction of force fields, simulations of

larger systems containing thousands up to tens of thousands of atoms can be simulated for large times. Today it is possible to develop a more accurate and flexible force field that can be used with general computer modelling method to predict properties for molecules in different environment. Best parametized force fields are able to predict molecular structures, conformational properties, and vibrational frequencies for isolated molecules. The force acting on atoms is obtained from the derivatives of the interatomic potential $V(\bar{r})$ is given by:-

$$\bar{F} = -\nabla V(\bar{r}) = -\frac{dV(\bar{r})}{d\bar{r}} \tag{10}$$

The interatomic potential $V(\bar{r})$ which is a function of position can be expressed as

$$V(\bar{r}) = \sum_{ij} V(r_i, r_j) + \sum_{ijk} V(r_i, r_j, r_k) + \sum_{ijkl} V(r_i, r_j, r_k, r_l) + \ldots \tag{11}$$

where the first term refer to the 2-body interaction the second term refers to the 3-body interactions, etc. In principle this could be continued up to N-body interaction term. The series is truncated and the significant terms represents effective interactions that incorporate higher terms in an average way. The interatomic potential can be written as

$$V(r, \theta, \phi) = \sum V_{bond}(\bar{r}) + \sum V_{nonbonded}(\bar{r}) + \sum V_{angle}(\theta) + \sum V_{dihedral}(\phi) \tag{12}$$

The potential depends on the interatomic distance r, the bond angle θ and the dihedral angle ϕ

2.6.1 Two body interaction

The first two terms in equation (12) describe the 2-body, bonded and non bonded interaction and depend on distance r between atoms. The bond vibrations are described by the harmonic potential

$$V_{bond}(\bar{r}) = \frac{1}{2} k_b (b - b_0)^2 \qquad (13)$$

where k_b = force constant for the bond and it controls the stiffness of the bond spring, while b_0 defines the equilibrium length.. Unique k_b and b_0 parameters are assigned to each pair of bonded atoms based on their types (e.g. C-C, C-H, C=C, C≡C, O-C, etc.). This equation estimates the energy associated with vibration about the equilibrium bond length and is based on Hooke's law.

2.6.2 Many body interactions

The third and the fourth term describe the interaction of more than two atoms. The angle vibrations are treated by a harmonic potential

$$V(\theta) = \frac{1}{2} k_\theta (\theta - \theta_0)^2 \qquad (14)$$

θ_0 is the equilibrium angle, k_θ is a force constant for bond and vibration. Unique parameters for angle bending are assigned to each bonded triplet of atoms based on their types (e.g. C-C-C, C-O-C, C-C-H, etc.). The effect of the k_b and k_θ parameters is to broaden or steepen the slope of the parabola. The larger the value of k, the more

energy is required to deform an angle (or bond) from its equilibrium value. Shallow potentials are achieved for k values between 0.0 and 1.0.

The 4-body dihedral rotation is described by a potential function of the form:-

$$V(\phi) = k_{\phi}[1 + \cos(n\phi - \delta)] \tag{15}$$

where k_{ϕ} is a force constant and it controls the amplitude of the curve, n is the multiplicity factor and it controls its periodicity, δ shifts the entire curve along the rotation angle axis ϕ. The torsion energy in molecular mechanics is primarily used to correct the remaining energy terms rather than to represent a physical process. The torsional energy represents the amount of energy that must be added to or subtracted from the Stretching Energy + Bending Energy + Non-Bonded Interaction Energy terms to make the total energy agree with experiment or rigorous quantum mechanical calculation for a model dihedral angle (ethane, for example might be used as a model for any H-C-C-H bond). The parameters are determined from curve fitting. Unique parameters for torsional rotation are assigned to each bonded quartet of atoms based on their types (e.g. C-C-C-C, C-O-C-N, H-C-C-H, H-C=C-H etc.).

2.6.3 Non-bonded interactions

Two atoms that are not bonded interact with each other through the non-bonded van der Waals' potential which consist of the Lennard-Jones potential

$$V(\bar{r}) = 4\varepsilon[(\frac{\delta}{r})^{12} - (\frac{\delta}{r})^{6}] \tag{16}$$

Where δ is the equilibrium distance and ε is the well depth of the potential, r is the distance between interacting atoms. When the distance is larger than the equilibrium distance the r^{-6} term dominates, corresponding to the long range attractive tail of the potential between the particles, usually explained as a result of induced dipole moment between the atoms**.** Repulsion occur when the distance between interacting atoms becomes even slightly less than the sum of their contact radii. Repulsion is modelled by an equation that is designed to rapidly increase at close distances (r^{-12} dependency). The δ parameter control the depth and position (interatomic distance) of the potential energy well for a given pair of non-bonded interacting atoms (e.g. C:C, O:C, O:H, etc.). In effect, δ determines the degree of "stickiness and hardness" of the Van der Waals attraction of the atoms. The energy term that describes attraction/repulsion provides for a smooth transition between these two regimes and for charged particle the electrostatic potential is added.

$$V(\bar{r}) = \frac{q_i q_j}{4\pi\varepsilon_0 r} \tag{17}$$

where ε_0 is the minimum energy of the function. $q_i q_j$ are charges on atom i and j. The electrostatic contribution is modeled using a Coulombic potential. The electrostatic energy is a function of the charge on the non-bonded atoms, their interatomic distance, and a molecular dielectric expression that accounts for the attenuation of electrostatic interaction by the environment (e.g. solvent or the molecule itself). Often, the molecular dielectric is set to a constant value between 1.0 and 5.0. A linearly varying distance-dependent dielectric (i.e. 1/r) is sometimes used to account for the increase in environmental bulk as the separation distance between interacting atoms increases.

2.7 Type of force field

The most important step for molecular dynamics simulation is the choice of the force field as it describes approximately the potential energy hypersurface on which the atomic nuclei move. There are many force fields available for use, several with unique functional forms. The main properties that define the quality of a given force field are the functional form and the parameters derived as constants in the potential function. It is important to carefully select the form of the potential to suit the type of system under study. All force fields consist of bonded and non-bonded interaction terms. The difference between the force fields is the exact terms that are used**.** The energy of a molecule is calculated as the sum of these bonded and non-bonded interactions where bond, angle, and dihedral (bonded, Coulumbic and Van der Waals (non-bonded) term are calculated separately.

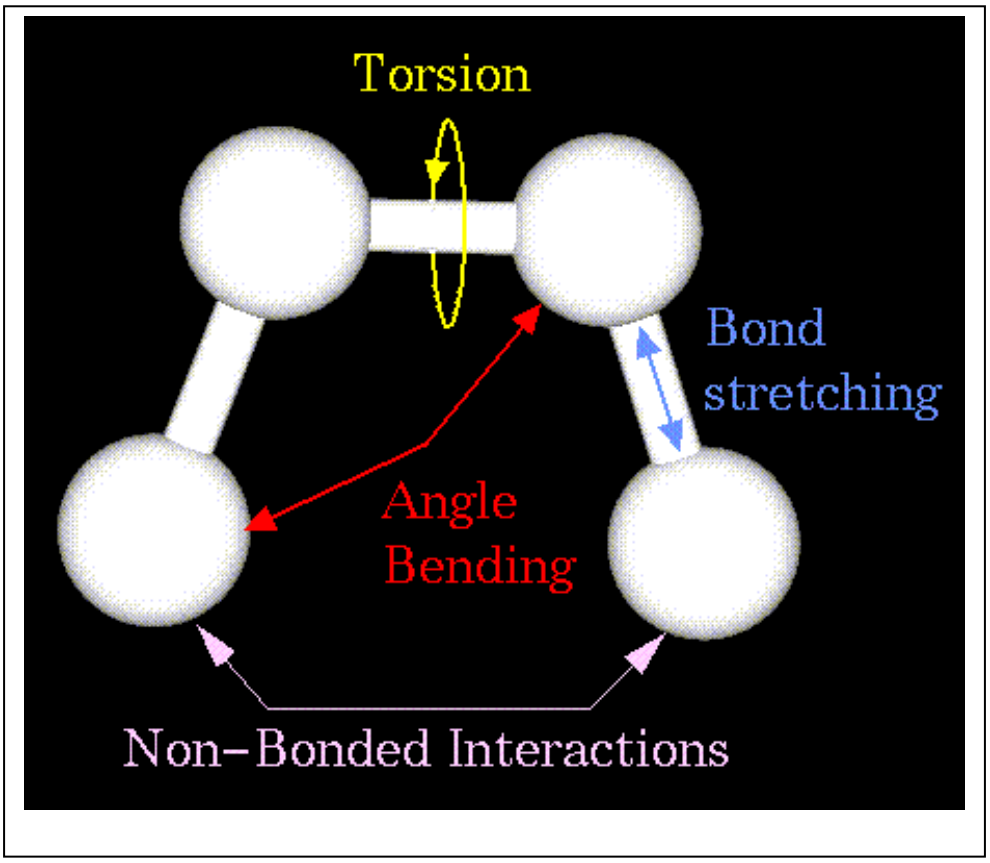

Figure 1 Schematic representation of the total energy of a system

Equations 10-14 are used by all of the early force fields. In the case of the bond stretch equation, later force fields used an extra cubic and sometimes a quartic term to more accurately describe the interaction, others use a totally different Morse function. Similar changes are made for the other bonded terms. The term which varies the most between force fields is the van der Waals term, it is usually a Lennard-Jones (LJ) 12-6 term but can be LJ 9-6* depending on the force field, in other cases the whole term is represented in a different form such as the Buckingham Potential.

2.7.1 COMPASS

Condensed-phase Optimizes Molecular Potential for Atomic Simulation Study (COMPASS) force field was derived from the Polymer Consistent Force Field (PCFF) force field using the hybrid approach consisting of both ab initio and empirical methods [36]. The nonbonded parameters were modified and consequently the valence parameters of PCFF were changed due to the coupling between the valence and nonbonded parameters, to construct a force field generally suitable for condensed-phase applications. It is a class II ab initio force field as it employs complex functional forms and is derived from extensive ab initio data. It is the first ab initio force field that was parameterized and validated using condensed phase properties (in addition to various ab initio and empirical data for molecules in isolation). It is specifically designed for material science application and it enables accurate and simultaneous prediction of structural, conformational, vibrational and thermophysical properties for a broad range of molecules e.g. most common organic molecules, organic and inorganic polymers, zeolites and metal/transition-metal

**LJ 9-6 is the soft Lennard-jones potential, which has a weaker repulsive term than the LJ 12-6*

oxides. However some of the functional groups required to model energetic materials have not until now been parameterized and included in the in the COMPASS force field

Parameterization method.

For all organic and inorganic covalently bonded molecules, including polymer, the Consistent Force Field (CFF) functional form is used. The total energy is written as a combination of valence terms including diagonal and off-diagonal cross coupling terms.

$$
\begin{aligned}
E_{valence} &= \sum_{b}\left[k_2(b-b_0)^2 + k_3(b-b_0)^3 + k_4(b-b_0)^4\right] \\
&+ \sum_{\theta}\left[k_2(\theta-\theta_0)^2 + k_3(\theta-\theta_0)^3 + k_4(\theta-\theta_0)^4\right] \\
&+ \sum_{\phi}\left[k_1(1-\cos\phi) + k_2(1-\cos 2\phi) + k_3(1-\cos 3\phi)\right] \\
&+ \sum_{\chi} k_2(\chi-\chi_0)^2 + \sum_{b,b'} k(b-b_0)(b'-b_0') + \sum_{b,\theta} k(b-b_0)(\theta-\theta_0) \\
&+ \sum_{b,\phi}(b-b_0)\left[k_1\cos\phi + k_2\cos 2\phi + k_3\cos 3\phi\right] \\
&+ \sum_{b,\phi}(\theta-\theta_0)\left[k_1\cos\phi + k_2\cos 2\phi + k_3\cos 3\phi\right] \\
&+ \sum_{b,\theta'} k(\theta-\theta_0)(\theta'-\theta_0') + \sum_{\theta,\theta'\phi} k(\theta-\theta_0)(\theta'-\theta_0')(\phi-\phi_0)
\end{aligned}
\tag{18}
$$

the valence term is formed by E_b, E_θ, E_ϕ and E_χ for bond, angle, torsion and out of plane angle coordinates respectively and $E_{bb'}$, $E_{b\theta}$,$E_{b\phi}$, $E_{\theta\theta'}$ and $E_{\theta\theta'\phi}$ for cross-coupling terms between internal coordinates. Cross-coupling terms are important for predicting vibrational frequencies and structural variations associated with conformational changes.

Two atoms that are not bonded interact with each other through the non-bonded potential which consist of the “soft” Lennard-Jones potential

$$E_{vdW} = \sum_{i,j} \varepsilon_{ij} \left[2\left(\frac{\delta_{ij}}{r_{ij}} \right)^9 - 3\left(\frac{\delta_{ij}}{r_{ij}} \right)^6 \right] \tag{19}$$

and the Coulombic term

$$E_{elec} = \sum_{i,j} \frac{q_i q_j}{r_{ij}} \tag{20}$$

for the electrostatic interaction. The electrostatic interaction is represented by the partial atomic charge model using bond increments, σ_{ij} which represents the charge separation between two bonded atoms. The net partial charge for atom, *i*, (q_i) is the sum of all bond increments over all atoms bonded to this atom

$$q_i = \sum_j \sigma_{ij} \tag{21}$$

E_{elec} refers to the electrostatic interactions between charged species/particles within a system. The two main areas of concern are firstly the description of the charge density and secondly the summation of the charge interactions. The interactions between two charges q_i and q_j separated by r_{ij} in a medium characterized with a dielectric constant ε_{ij}.

2.7.2 Dreiding force field

Dreiding force field [37] is a common method used to speed up MD calculations. It is a good, robust, all purpose force field. It uses the concept of united atom where

several atoms are modelled as one united atom of a mass equal to the combined mass of the atoms in approximation to reduce simulation time. The reason for this is twofold. First it reduces the number of atoms to be simulated, second, it enables the use of a larger time step in the integration scheme. CH_3 group is modeled as one united atom and we don't have to explicitly simulate the fast motions of the H-atom, but only at average way. This has an effect of eliminating the calculations of nine vibrations at each time step. The use of united atoms induces one artifact. For non-bonded interaction of united atoms with atoms separated by three covalent bonds (third neighbours) the repulsions are too large. In order to avoid this effect the van der Waals parameters used in the calculation of the third neighbour interaction are smaller than normal. A refinement on the approximation is the `anisotropic' united atom approximation where (for example in the case of polydimethylsiloxane) the center of the united atom is shifted away from the center of the carbon atom it is replacing in the direction of the two hydrogens and this gives good diffusion results. The disadvantage of Dreiding force field is that, it is a general (not a specialized) force field so it is less accurate as compared to specialized force field but it allows reasonable predictions for a very much larger number of structures, including those with novel combinations of elements and those for which there is little or no experimental data. It can be used for structure prediction and dynamics calculations on organic, biological, and main-group inorganic molecules

2.8 Charge description

This section deals with the way in which the charge distribution in a system may be represented.

2.8.1 Formal charges

Formal charges are atom centered charges of integral value and have been used with a great deal of success especially in ionic systems where the assumption of formal charges is at its most reasonable, however the more covalent character in a system, the less valid such an assumption becomes and although properties such as the structure may still be reproducible in such cases due to errors being subsumed in fitting of the parameters it may prove difficult to reproduce complex properties which require the correct balance between all the terms in the system.

2.8.2 Partial charges

Partial charges are normally centered and may take any value both integer and non-integer. These are described in two ways: fixed charges and bond increment charges.

2.8.2.1 Fixed charges

In the case of fixed charges the partial charge for a given atom in a given environment is uniquely defined. This is perhaps the most accurate of the two models however it requires a knowledge of the partial charge of every atom in the every environment; making it unwidely and impracticable for large force fields if they are to be used on a new systems.

2.8.2.2 Bond increment charges

This method requires the summation by bond increment in which the effect of a given atom type bonding to another atom type may be given. These can then be summed over all bonds for a given atom to produce consistent partial charge for an atom. This is not perhaps the most accurate as the unique partial charges model but it has the

advantage of requiring less parameters and not relying on the specific knowledge of the atomic environment.

2.9 Charge summation methods

The summation of atomic charges in a system is a question that has been studied extensively. The interaction of the two single point charges may be summed as described by equation (20) and (21). where ε_{ij} is the dielectric constant of the medium and r_{ij} is the inter-charge distance However when a system with many charges is considered the subject of summation becomes more complex, since the simple sum may require complex techniques in order to obtain an accurate value for coulombic energy of the system. The most commonly techniques of the summation are described in the following sections.

2.9.1 Atom based summation

Atom based summation of the charges is as the name suggests a simple summation of the electrostatic interactions of all the atoms within a given distance of each other.

This method has the advantage of being computationally inexpensive however the answer is only conditionally convergent; the method yield results that fluctuate dramatically as the cutoff increases, even at large cutoff values this is because the method is conditionally convergent. It is suitable for small systems where a large enough cutoff can be use so that the interactions between all atoms in a system can be considered.

2.9.2 Group based summation

The grouped based summation method relies upon the definition of neutral groups and the switching atoms within these groups. The groups are either included or dispensed with depending upon the distance between the switching atoms. The advantage of this method is that dipoles are not broken at the cutoff.

2.9.3 Ewald summation

Ewald summation involves the multiplication of the lattice sum by a convergence functions, allowing the convergence to be improved by doing so. In most cases the potential is described as a function of the inter-atomic distance r_{ij}. Some of the methods are described in the following section.

2.10 Buckingham potential

The Buckingham potential has been used successfully in many ionic systems.

The form of the potential is given by:

$$E_{elec} = A\exp\left(\frac{-r_{ij}}{\rho}\right) - Cr^{-6} \qquad (22)$$

The function includes three parameters A, ρ, and C. A and ρ describe the repulsive of the component of the potential, which is an exponential rather than power function and gives arguably a better reproduction of the repulsive term. C is the attractive or dispersive interaction due to induced dipole interactions. This analytical form is not conformal and therefore does not allow for combination of parameters by combining rules as do the Lennard-Jones potential. A further disadvantage is that at very short

distances the function approaches minus infinity with the catastrophic results for any model approaching such short distances. Finally it should be noted that evaluation of this exponential form is relatively expensive compared to power laws as the Lennard-Jones function.

2.11 Lennard-Jones Function

The Lennard-Jones function/potential has been used in a widely variety of modelling techniques and for variety of systems. Its main strength lies in its simplicity of form. It is both computationally inexpensive since it is a simple power law and readily transferable because it conformal allowing the combining of parameters, allowing the production of heteronuclear parameters from homonuclear. There are equally popular and identical forms for expressing Lennard-Jones potential. The first form has two parameters A and B and the second form also has two parameters ε and δ which represent the well-depth and equilibrium distance respectively

$$E_{vdw} = \left(\frac{A_{ij}}{r_{ij}}\right)^{12} - \left(\frac{B_{ij}}{r_{ij}}\right)^{6} \tag{23a}$$

$$E_{vdw} = \varepsilon_{ij}\left[\left(\frac{\delta_{ij}}{r_{ij}}\right)^{12} - \left(\frac{\delta_{ij}}{r_{ij}}\right)^{6}\right] \tag{23b}$$

The conversion between the parameters is given in equations below

$$\varepsilon_{ij} = \frac{1}{4} A_{ij} B_{ij}^{2} \tag{24a}$$

$$\delta_{ij} = \sqrt{2\frac{A_{ij}}{B_{ij}}} \tag{24b}$$

$$A_{ij} = \delta_{ij}^{12}\varepsilon_{ij} \tag{24c}$$

$$B_{ij} = 2\delta_{ij}^{6}\varepsilon_{ij} \tag{24d}$$

Power Rule

The Lennard-Jones potential was chosen for the analytical simplicity of the function and it is characterized into two forms namely: the 12-6 potential is a steep repulsive potential and 9-6 potential which shallower repulsive term. The two forms of the potential are given below:

$$E_{vdw} = \left(\frac{A_{ij}}{r_{ij}}\right)^{9} - \left(\frac{B_{ij}}{r_{ij}}\right)^{6} \tag{25}$$

The conversion between equations 19 and 25 is shown below:

$$\varepsilon_{ij} = \frac{4}{9}A_{ij}^{2}B_{ij} \tag{26a}$$

$$\delta_{ij} = \left[\frac{3A_{ij}}{2B_{ij}}\right]^{\frac{1}{3}} \tag{26b}$$

$$A_{ij} = 2\delta_{ij}^{9}\varepsilon_{ij} \tag{26c}$$

$$B_{ij} = 3\delta_{ij}^{6}\varepsilon_{ij} \tag{26d}$$

Combining rules

One of the advantages of the Lennard-Jones potential is that it is conformal, that it is possible to combine the parameters for two atoms to produce those for the interactions between the two interacting different atoms. There are three commonly used sets of rules for these combinations: arithmetic, geometric, and sixth-power

Arithmetic

$$\varepsilon_{ij} = \sqrt{\varepsilon_{[i^2]}\varepsilon_{[j^2]}} \tag{27a}$$

$$\delta_{ij} = \frac{\left(\delta_{ii} + \delta_{jj}\right)}{2} \tag{27b}$$

Geometric

$$\varepsilon_{ij} = \sqrt{\left(\varepsilon_{ii}\varepsilon_{jj}\right)} \tag{28a}$$

$$\delta_{ij} = \sqrt{\delta_{[i^2]}\delta_{[j^2]}} \tag{28b}$$

Sixth Power

$$\varepsilon_{ij} = \sqrt{\left(\varepsilon_{ii}\varepsilon_{jj}\right)^{\frac{1}{2}} 2\frac{\delta_{ii}^{3}\delta_{jj}^{3}}{\delta_{ii}^{6} + \delta_{jj}^{6}}} \tag{29a}$$

$$\delta_{ij} = \frac{\left(\delta_{ii}^6 + \delta_{jj}^6\right)^{\frac{1}{6}}}{2} \tag{29b}$$

Mathematical properties of combining rules are considered and it is shown how to reduce combining rule formulas from a two-parameter to a single-parameter problem.

2.12 Calculation of temperature pressure and volume

Newton's equation of motion conserves the total energy of a system and therefore it is characterized by micro-canonical statistical mechanical ensemble. The temperature of the system is calculated using the average kinetic energy of the N particles with N_f degrees of freedom

$$\frac{1}{2} k_b N_f T = \sum_{i=1}^{N} \frac{1}{2} m_i v_i^2 \tag{30}$$

where v_i the velocity of particle i with mass m_i the temperature of the simulated system is controlled by the use of a weak temperature and /or pressure coupling to an external bath. This means that at each integration step the velocity v are scaled to λ_v with

$$\lambda = [1 + \frac{\Delta t}{\tau_T} (\frac{T^{ref}}{T(t - \frac{1}{2}\Delta t)} - 1)]^{\frac{1}{2}} \tag{31}$$

to bring the temperature of the system $T(t-\Delta t)$ towards the reference temperature (T^{ref}). The time constant τ_T describe how tight the coupling is. A tight coupling

($\frac{\Delta t}{\Delta \tau_T}$) $\geq$ 1, means that there is little fluctuation around the T^{ref}. The expression for pressure of the system is based on the virial theorem of the form:

$$\frac{PV}{kT} = \sum_{i=1}^{\infty} a_i(T)\left(\frac{\lambda^3}{\nu}\right)^{i-1} \tag{32}$$

where $\nu = \frac{V}{N}$ denotes the volume per particle in the system, $a_i(T)$ is the virial coefficient.

CHAPTER 3

COMPUTER SIMULATION

In this chapter emphasis will be put on structure generation and refinement from which molecular dynamics was performed.

Molecular Dynamics reported on this thesis were performed using *Amorphous builder module of Cerius*[2] package. This uses a standard Monte Carlo method (which is based on the use of random numbers and probability statistics to investigate problems) that creates the polymer site using energy at specified temperature and density.

3.1 Generation of amorphous structure

3.1.1 Overview

In order to model penetrant/polymer permeation accurately one must first be able to model the polymer itself. Computer simulations have often been used to model small regions of liquid in full atomistic detail. The extension of this method to polymers has proven difficult due to the wide range of length-scales and relaxation time scales present within a polymer that are absent in liquids. A single polymer chain shows structures ranging from the chemical bond (Å) to the persistence length (10Å) through to the coil radius (100Å). The time-scales range from local conformational fluctuations in the nanosecond region to fluctuations of the end-to-end distance that are in the order of seconds [38]. Nonetheless, various techniques have been employed to create a model of a suitable amorphous polymer, the most common of which are discussed below.

The methods discussed can be broadly split into three distinct types:

- Structure generation - emphasis is on the generation of the initial structure leaving subsequent refinement to a minimum
- Structure refinement – emphasis is on the refinement which, ideally, is so good that the starting structure can be arbitrary
- Coarse graining – mapping the atomistic model on to a lattice model, and then mapping back after relaxation of the coarse grain model.

It is difficult to state which of the following methods can be described as the 'best' since all have particular advantages and disadvantages.

3.1.2 Structure generation methods

One common method of producing an amorphous polymer is the self avoiding random walk. This employs sequential site-by-site generation of the chain, including the effects of excluded volume and intramolecular potentials. The co-ordinates of successive polymer units are calculated using the equilibrium bond length and valence angles but at random dihedral angles. The energy change caused by the introduction of the new site is calculated and the move is accepted or rejected by a Monte Carlo type criterion. This method has been criticized for its simplistic approach to the problem [39]. One objection is that the initial chain configurations are generated in vacuo such that no interactions between chain are taken into account. The subsequent minimization techniques used cannot be expected to overcome this in the time available due to large relaxation times present within the polymer as mentioned previously. Also, this method is not practical to generate polymer at high densities

since the probability of finding a suitable site tends to zero as the simulation cell become increasingly full.

An improvement is phantom chain growth without excluded density, which was devised to create higher density polymer [40, 41]**.** Here all excluded volume effects are ignored apart from those separated by three sites since, following Flory's theory [42], the assumption is made that the polymer melt chain structure is largely determined by the localised intramolecular interections. A consequence of this method is large number of overlapping atoms. Energy minimization would remove these overlaps but this effectively means that the structure is quenched to 0K and this could potentially cause a shift in the distribution of conformers. Instead molecular dynamics techniques are preferred whereby van der Waals potentials are introduced and the structure undergoes molecular dynamic simulation. However, if the full Lennard-Jones potential is used at this stage, enormous forces are generated between atoms that can cause the integration algorithm to breakdown. To avoid this situation, the Lennard-Jones potential is modified to be constant below some critical separation. This ensures that overlaping atoms are pushed apart gently and that the forces are not excessive. It has been reported that, despite this precaution, the sudden introduction of the forces can cause significant perturbations in the chain dimensions. Once all the pairs of atoms are separated by distance greater than a critical separation, the full Lennard-Jones potential is invoked.

A method that has proved to be more popular is based on rotational isomeric state (RIS) theory [43] whereby the initial structure is generated such that it satisfies the known probability of dihedral angles within the chain at a given temperature. Unlike

the above methods, RIS takes in to account the long-range interactions (separated by 5 or more atoms) which are thought to have important effects in polymers of high densities. This tends to produce an initial guess configuration that is of significantly lower energy than those of previous methods. The model is then relaxed by minimising the potential energy. This method of producing the polymer configuration has been used extensively within the literature, though it is usually in its modified form of having periodic boundary conditions.

A common problem of the RIS method occurs when large monomers are used. Severe overlaps of atoms occur during the initial guess configurations which results in a great deal of energy minimisation needed to relax the structure. A novel solution to this is the method of in-situ polymerization [44]**.** Here the configuration of monomers is generated in the small box. Molecular dynamics at the elevated temperature is used to randomly orientate the monomers after which adjacent monomers are joint and the resulting polymer undergoes energy minimisation. This does ensure that no atoms overlap but cannot guarantee a statistically accurate distribution of dihedral angles [45]**.** Further complications arise when a desired tacticity or monomer sequence is required.

A recent implementation of a Monte Carlo algorithm is "look-head" method [46] which, before allowing a particular placement of the next atom, calculates what the energies several steps ahead would be averted a few step earlier than when a "look-head" is not used. Obviously, a too large a look-head will result in a very high computational time. A typical value for the look-head is between two and four bonds.

3.1.3 Structure refinement methods

Instead of trying to produce a realistic amorphous polymer immediately, one can use structure refinement techniques to turn an arbitrary starting configuration into a realistically amorphous one. One such method is that of reptation Monte Carlo [47] where a chain reptation movement is mimicked by removing a monomer unit from one end of a chain and attaching it to the other end. Choosing a dihedral angle at random and using equilibrium bond length and valence angle generates the new site for the monomer unit. The change in energy is calculated and the Monte Carlo rules are used to accept or reject the new site.

Another structure refinement method is that using standard molecular dynamic techniques but with non-physical force field [48, 49]. The starting configuration is of dilute chains contained in a periodic box interacting through normal bonded forces. A soft core repulsive potential is then used during molecular dynamics whilst the simulation box is compressed to experimental density. This has the effect of allowing atoms to pass each other, thus enabling the chains to become entangled. If van der Waals forces were included at this point the chains would merely be pressed together. When the required density is reached conventional energy minimization is used with the full force field.

3.2 Coarse-graining method

The general idea of a coarse grain method is to map the initial structure onto a lattice model, mapping back to the atomistic level once the correct structure has been generated. An example [45] guarantees Gaussian chain statistics, enables control of chain tacticity and monomer sequence and avoids severe atomic overlap. A trajectory is generated by self avoiding walk on completely occupied lattice model. This

trajectory becomes the polymer backbone and is then populated by the desired atoms according to the specific chemical structure of the polymer. Correct placement and orientation of the atoms avoid atomic overlap and sequence in which the atoms are placed on the lattice determined monomer sequence and tacticity. Only brief energy minimization is needed to relax the structure and molecular dynamics is used to remove the lattice periodicity, resulting in a structure that has been shown to reproduce experimental x-ray scattering patterns.

3.3 Simulation of amorphous polydimethylsiloxane

All polymer systems were generated using the Amorphous Polymer Builder of Cerius2, which implements the RIS theory to select the torsional distributions from specified gauche-trans barriers. A cell that contains a PDMS chain of 200 monomers with cubic periodic boundary conditions has been used to investigate the diffusivity of twenty PDMS cyclic oligomer D3, D4 and D5 as shown in figure 2 at prescribed temperatures. The building procedure was followed by energy minimization of 3000 steps to remove occasional bad contacts which lead to non bonded energies between atoms that happen to be close. Then the structure was equilibrated for 200ps. The equilibration process was followed by 5000ps of production.

3.4 Structures

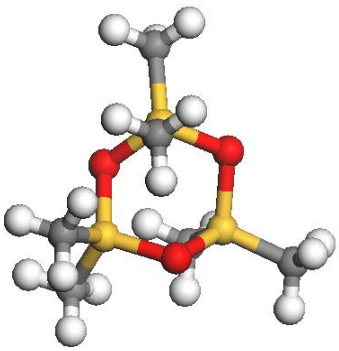

Figure

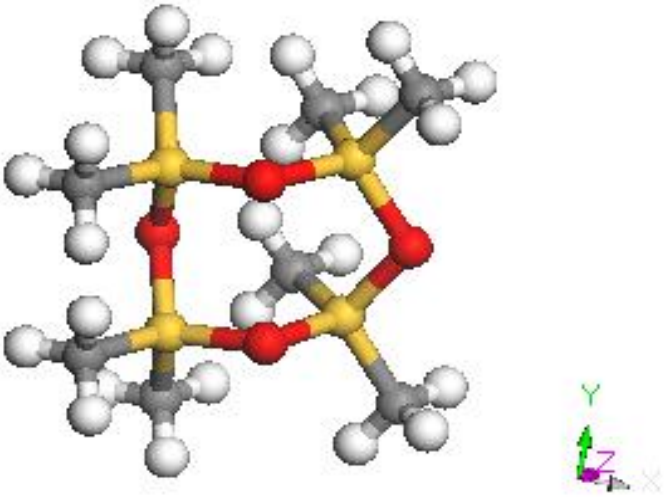

Figure 3, octa-methylcyclotetrasiloxane (D4)

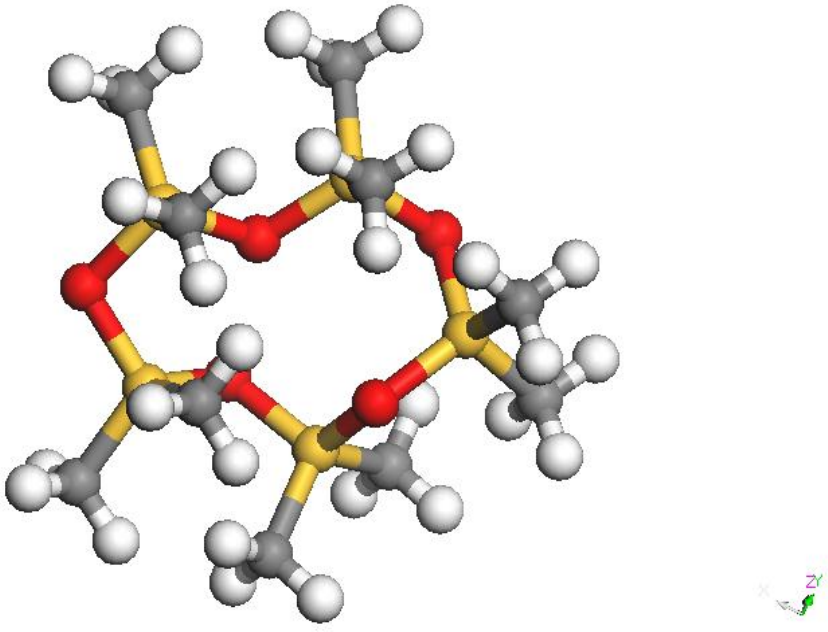

Figure 4, deca-methylcyclopentasiloxane (D5)

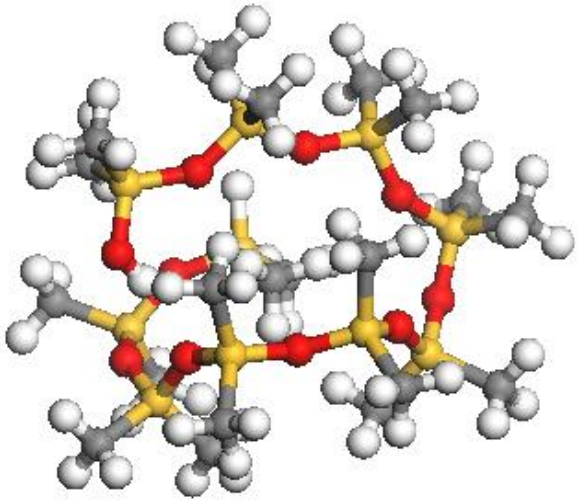

Figure 5, PDMS chain consisting of 10 monomers

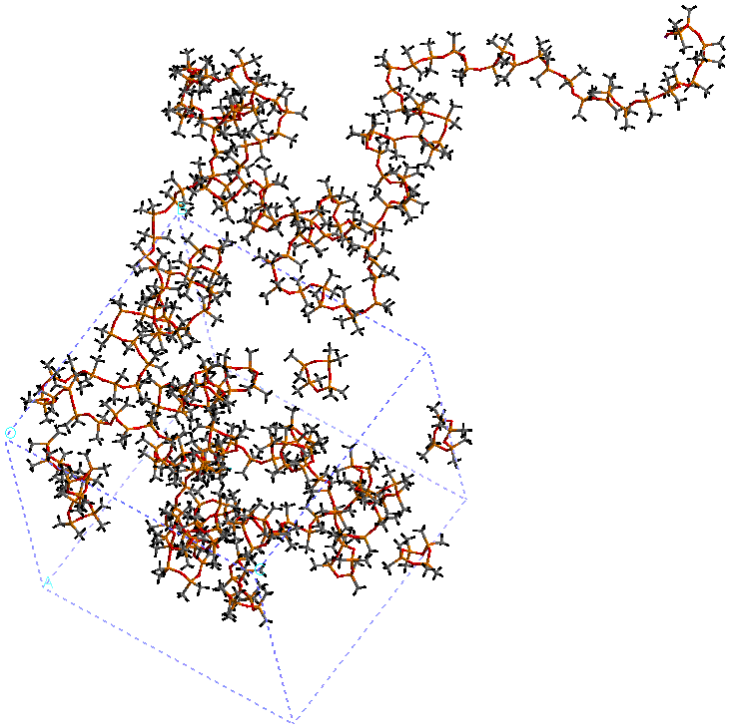

Figure 6, 3D periodic system containing 20 D4 penetrants and a PDMS polymer chain consisting of 200 monomers.

3.5 Energy minimization

The most common way of refining a structure is by energy minimization. It is a useful method in bringing a molecule close to its equilibrium conformation. It can repair distorted geometries by moving atoms to remove internal constrains. The aim of energy minimization is to find a local energy minimization, i.e., the bottom of the energy well occupied by the initial conformation. The local energy minimization locates the nearest point of stability on the potential energy surface. At such a point, the net force on each atom given by the derivative of the energy function, is zero. For small molecules, a global minimum energy configuration can often be found; for large macromolecular systems, energy minimization allows one to examine the local minimum around a particular conformation. Energy minimization is often performed in order to relieve strain in experimentally obtained or averaged structures. In addition, barrier crossing or internal rearrangement in very large macromolecules may be studied through a combination of minimization techniques and coordinate constraints.

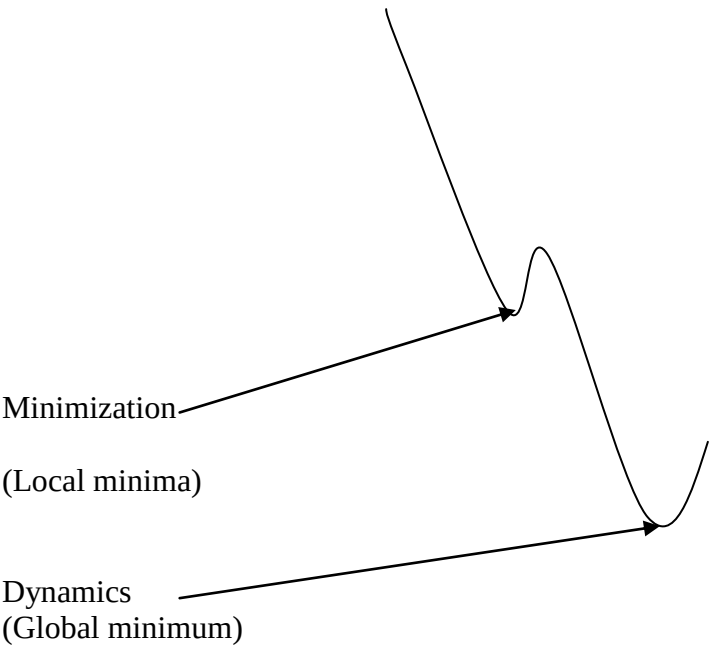

3.6 Molecular dynamics

Molecular dynamics (MD) is a convenient way to shake a molecule from one local energy minimum to another. It applies the laws of classical mechanics to compute the motion of the particles in a molecular system. This allows the study of molecular and conformational stability, the likely effects of flexibility on reactions or properties, the thermally averaged molecular structure, and any other property dependent upon molecular motion - examples include diffusion, permeability, binding mechanisms, and vibrational modes. Molecular dynamics alters the intramolecular degrees of freedom in a step-wise fashion, analogous to energy minimization. The individual steps in energy minimization are directed at establishing a down-hill direction to a minimum. The steps in molecular dynamics, on the other hand, represent the changes in atomic position, r_i, over time (i.e. velocity) [37].

MD is mostly suitable to study transport of small molecules in a material matrix. However if jump events of larger molecules can occur within time frames accommodated by MD, it could be applicable as well.

3.7 Calculation of the diffusion

Diffusion in polymeric systems is passive, the driving force is purely a Brownian molecular motion, but diffusion can also be activated by external effects, either by the influence of the release medium by swelling or biodegradation, or by the effects of physical forces as electrical, osmotic or convective forces. The fundamental of diffusion is based on Fick's laws which describe the macroscopic transport of molecules by a concentration gradient.

$$J = -D\frac{dC}{dx} \tag{33}$$

where J is the flux of particle, D is the diffusion coefficient, C is the concentration. This law holds in case of thermal and mechanical equilibrium. The first Fick's law is a pertinent modelisation for a steady state diffusional release. Fick's model is adapted to passive diffusional systems where the diffusion coefficient (D) may be supposed to be constant, without modification of the physico-chemical properties of the polymer during the release. Such systems are so-called Fickian systems [50].

Diffusion in polymers

In a microscopic picture, the diffusion coefficient is related to the autocorrelation function of the particle current by

$$D = \frac{1}{3}\int_0^\infty < [\sum_i^N \bar{v}_i(0)][\sum_j^N \bar{v}_j(t)] > dt \tag{34}$$

the sum extend over all N particles**,** i **,** in the system, and the angle brackets imply the ensemble average. If the concentration of the diffusing species is low and the interaction between these particles is short-range, then one can approximate that the velocities of two different particles, i and j, are uncorrelated, i.e. $< \bar{v}_i(t)\bar{v}_j(0) >= 0$.

Hence equation (34) becomes

$$D = \frac{1}{3}\int_0^\infty < \bar{v}_i(t)\bar{v}_i(0) > dt \tag{35}$$

this equation is known as the Green Kubo relation for the diffusion coefficient and it states that the diffusion coefficient is given by the time integral of a single-particle

centre of mass velocity autocorrelation function. If the simulation is long enough for the hydrodynamic limit (long time limit) to be reached, equation (35) can be shown to be equivalent to the Einstein equation

$$6Dt = < \left| \overline{R}_i(t) - \overline{R}_i \right|^2 > \tag{36}$$

$\left| \overline{R}_i(t) - \overline{R}_i(t) \right|^2$ is the centre-of-mass mean-square displacement (MSD) which is the square displacement a particle has moved from time $t = 0$ to t. The particle's cartesian position vector is denoted by $\overline{R}_i$. Equation (36) implies that in the long-time limit the MSD is proportional to the time elapsed. Equations (34), (35) and (36) are completely equivalent in the calculation of the diffusion coefficients from the microscopic motion of individual particles. The resulting diffusion coefficients are often called tracer diffusion coefficients. Einstein equation (36) holds only in the case that the observation time is large enough to allow the particle to show completely uncorrelated motion, i.e. the particle has no memory of previous steps. This means that MSD is linear with time. However at shorter time scales, the motion might be correlated, which implies that equation (36) is not valid, hence the diffusion coefficient cannot be defined. Different cases can be summarized as follows:

- the MSD is quadratic in time $< \left| \overline{R}_i(t) - \overline{R}_i \right|^2 > \alpha t^2$. This is equivalent to the displacement being linear in time which is the signature of free flight. In a dense system, it occurs only at very short time scales (<1ps) while the particle is moving freely within a cavity until it hits the cage wall.
- MSD is linear in time $< \left| \overline{R}_i(t) - \overline{R}_i \right|^2 > \alpha t$. The motion of a particle is uncorrelated, satisfies equation (36)

- $< \left| \overline{R}_i(t) - \overline{R}_i \right|^2 > \alpha t^n, n < 1$. This is the case of anomalous diffusion. It is caused by some environmental features which prevents the particle from perfoming an uncorrelated motion.
- $< \left| \overline{R}_i(t) - \overline{R}_i \right|^2 > \alpha t^n, n > 1$, this is called superdiffusion, can occur if some other transport mechanism such as convective flux is superposed to the diffusion.

CHAPTER 4

RESULTS AND DISCUSSIONS

This chapter the results obtained from simulations will be analyzed and discussed, where applicable, the results will be compared with those available.

4.1 Diffusion in polymer

The study of the dynamics of small molecules in polymer melts has focused to a large extent on the calculation of diffusion coefficients D of these molecules. The diffusion coefficients are obtained from the mean square displacement $< \left| \overline{R}_i(t) - \overline{R}_i \right|^2 >$ of these molecules or the time integral of the velocity auto-correlation function obtained from the trajectories. In low molecular weight liquid, the diffusion regime characterised by

$$6Dt = < \left| \overline{R}_i(t) - \overline{R}_i \right|^2 >$$

sets in after a few picoseconds. In polymer melts however a small molecule diffuses by a completely different mechanism namely by performing a jump-like motion between low free energy sorption sites.

The mean square displacement method is preferred over the velocity autocorrelation function because the latter tends to become noisy at larger t and it is often necessary to make assumptions about the analytical form of its long time tail in order to calculate the integral unless excessive simulation time is spent [52]. The Einstein relation avoids such ambiguity, secondly in the leap-frog integration scheme, the atom velocities are first calculated at time, $t + \frac{1}{2}\delta t$, these are used to calculate the positions,

r, at time, $t + \delta t$. The mean square displacement is not determined by the short time behaviour as is the Green-Kubo relation and trajectory frames have to be saved to disk less often. Finally to verify if the hydrodynamic limit has been reached or if anomalous diffusion prevails, the graph of log MSD versus log time is plotted and the slope of the graph will give the value of n as discussed in section 3.7.

4.2 Analysis

4.2.1 Motion of penetrant

As a first step in molecular dynamics evaluation, the movement of simulated penetrant molecules through the polymer is usually characterised quantitatively and qualitatively [19, 39, 53-58]. The simplest way of studying the diffusion of an individual penetrant is to look at its path through space. This can be done by analysing the displacement versus time graph which reveals much about the motion of penetrant as shown in figures 7-9**.** From theses graphs, the motion of small molecules in a polymer can be characterised into two categories, penetrants hopping in a cavity, and penetrant jumping from one cavity to another [59]

4.2.1.1 Hopping mechanism

Penetrants spend larger part of time in cavities. These residence period do not contribute to diffusion but they are quite interesting in their own right. The motion of penetrants trapped in a cavity is dominated by short time scales [60], typically less than 0.5ns. During this quasi-stationary period, penetrant are reflected by the polymer matrix [61]. In this mode of motion, the penetrant molecules also act as probes for the shape of visited free volume [59]. After this time, most of the correlation of molecular

motion is lost due to frequent collision with the polymer atoms forming the cavity walls.

4.2.1.2 Jump event

During a jump event, a penetrant moves from a cavity it resides in, to a neighbouring cavity in a very short time compared with the residence time. Looking at the displacement vs time graph (figure 7-9)**,** it reveals some difference in motion patterns which are mainly related to the size of the penetrants, D3-D5. Figure 7 shows the motion of a D3 penetrant diffusing through a PDMS polymer. The hop and jump kind of motion is not clear as compared to that in figure 8 and 9.The penetrant seems to spend less time in a cavity, compared to that of figure 8 and 9. The diffusion seems not limited by the number of cavities available to the penetrant in a polymer matrix and their distribution but seems to be limited by the mobility of the polymer matrix. However in figure 8, which shows the motion of D4 penetrant in PDMS, the step like-jump motion is clear. The penetrant seems to spend more time (compare to figure7) oscillating in a cavity, approximately 0.5ns, as can be clearly seen in the intervals, 3000-3500ps; 3500-4000ps and 4000-4500ps. From time to time the penetrant finds a channel big enough to jump to the adjacent cavity in a very short time compared to the residence time. This jump event can be clearly seen at approximately 4000ps and 4500ps. In figure 9 which shows the motion of a D5 penetrant in PDMS polymer, the step-like motion is also clear. The penetrant spent more time in a cavity it resides in, approximately 1ns, as can be clearly seen in the intervals 2000-3000ps and 3000-4000ps. From time to time a penetrant jumps from one cavity to another in a very short space of time as can be seen at 2000ps, 3000ps and 4000ps. The analysis of the penetrant trajectory thus demonstrates a variation in the diffusion with respect to

penetrant size. For larger penetrants the more pronounced events are the step-like hops and jumps as can be seen in figure 8 and 9. Penetrants (D4) hop within a cavity for approximately 0.5ns and after that it jumps to the next cavity. However, for D3 penetrant, which is the smallest; these step-like hops appear to be blurred to some extent. One may wonder, if penetrants smaller than D3 would have displacement curves completely without steps, which would be indicative of a diffusion mechanism without discrete jump events. The residence time also differs with respect to penetrant size; for larger penetrants the residence time is longer and this is shown in figures 8 and 9. The time spent by D5 penetrant in one cavity is approximately 1ns where as for D4 is approximately 0.5ns. This confirms that diffusion in polymers is determined by jump events.

The question arises, what atomic motions are involved in the jump events, and, in particular, how does the polymer matrix participate in the event or even facilitate it. F. Muller-Plathe [39] repeatedly attempted to relate jump events to sudden conformational changes in the polymer and also to the major torsional angle changes and ring flips but could not find any correlation. It appeared rather that many degrees of freedom of the polymer are involved in a distributed fashion. The thermal vibrations of the polymer matrix do then, from time to time, permit the formation of temporary channels between adjacent cavities. These connections can under suitable conditions be utilized for jumps of a diffusing particle from one hole to a neighbouring one.

As discussed above, one can clearly identify the very fast oscillations inside one and the same cavity as can be seen in time interval 3500-4000ps (figure 8) and the distinctive jumps between different cavities in a very short space of time. The short

frequency oscillations with amplitudes of less than 0.3 Å (figure 8) correspond to movements inside a given void in a polymer matrix, while larger once, more than 0.3 Å can be related with the jump event between two adjacent holes. At about 4100 and 4500ps, the jumps are so high that the diffusing particle might have jumped more than one cavity.

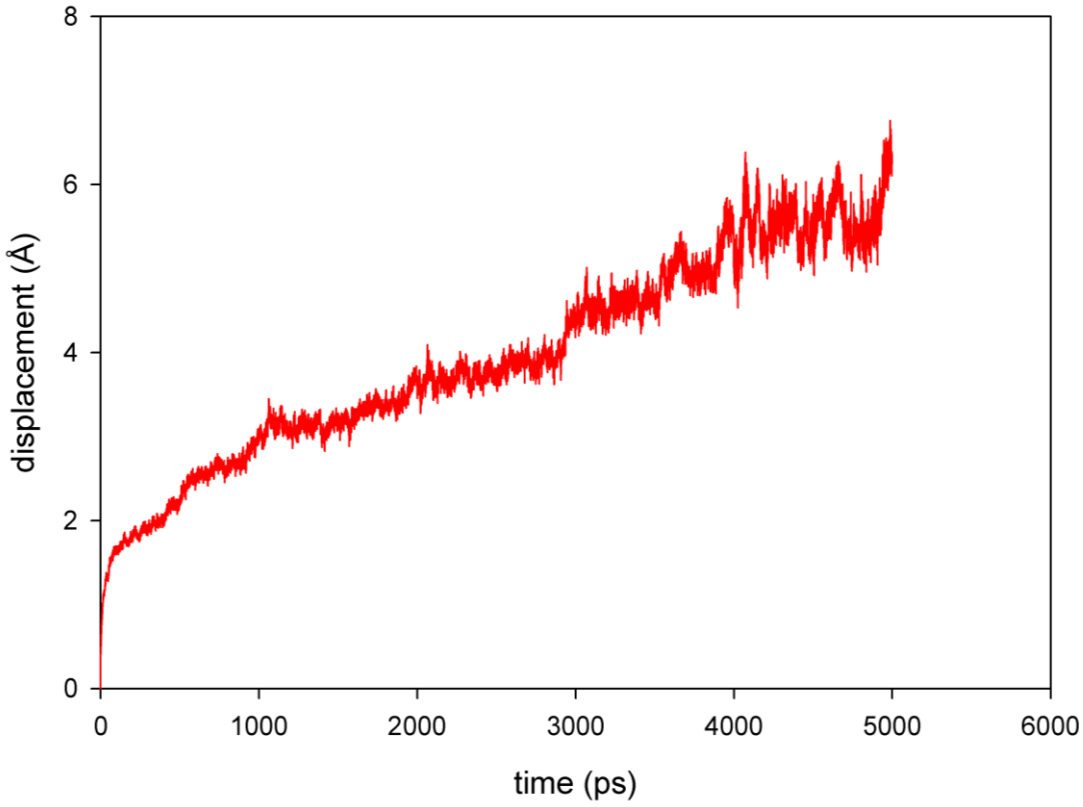

Figure 7, The variation of the displacement with time for a D3 penetrant at 300K using Dreiding *force field*

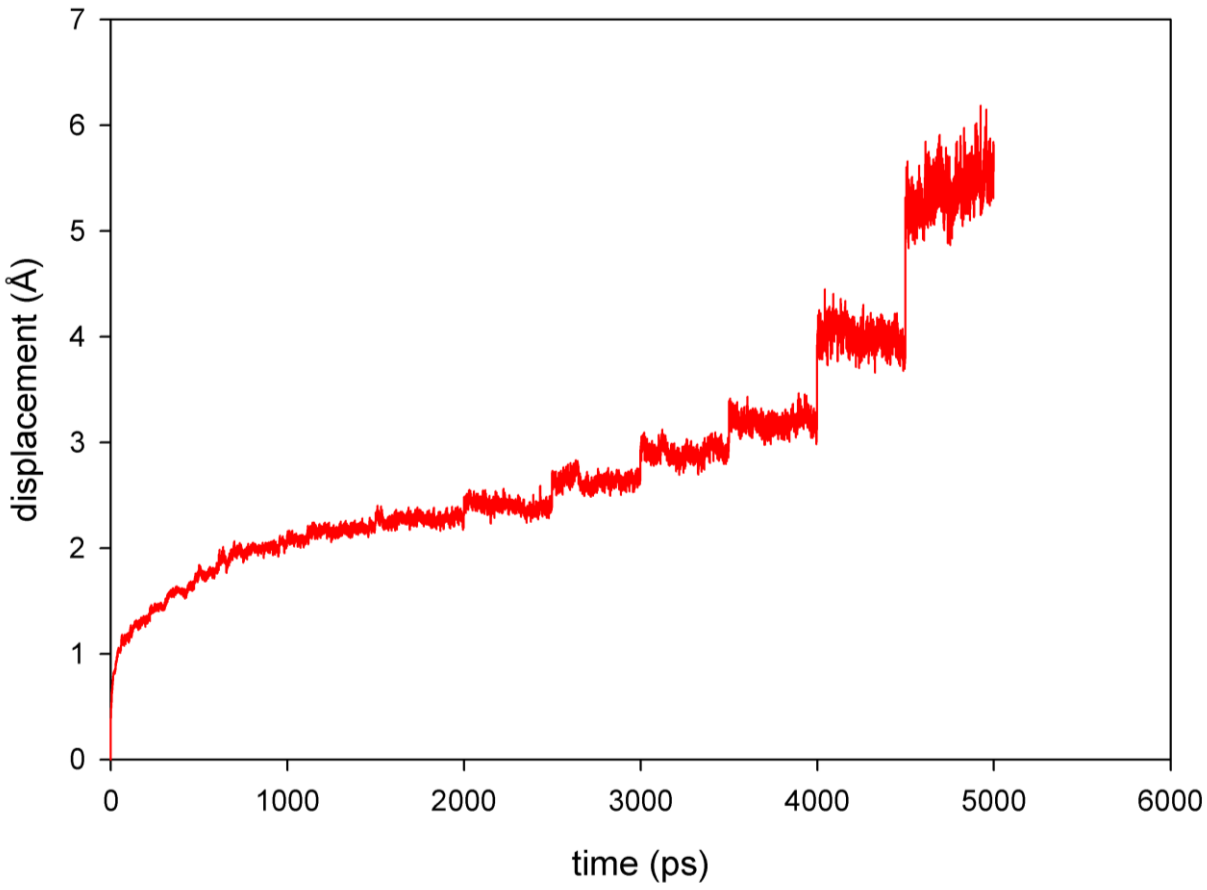

Figure 8, The variation of the displacement with time for a D4 penetrant at 300K using Dreiding *force field*

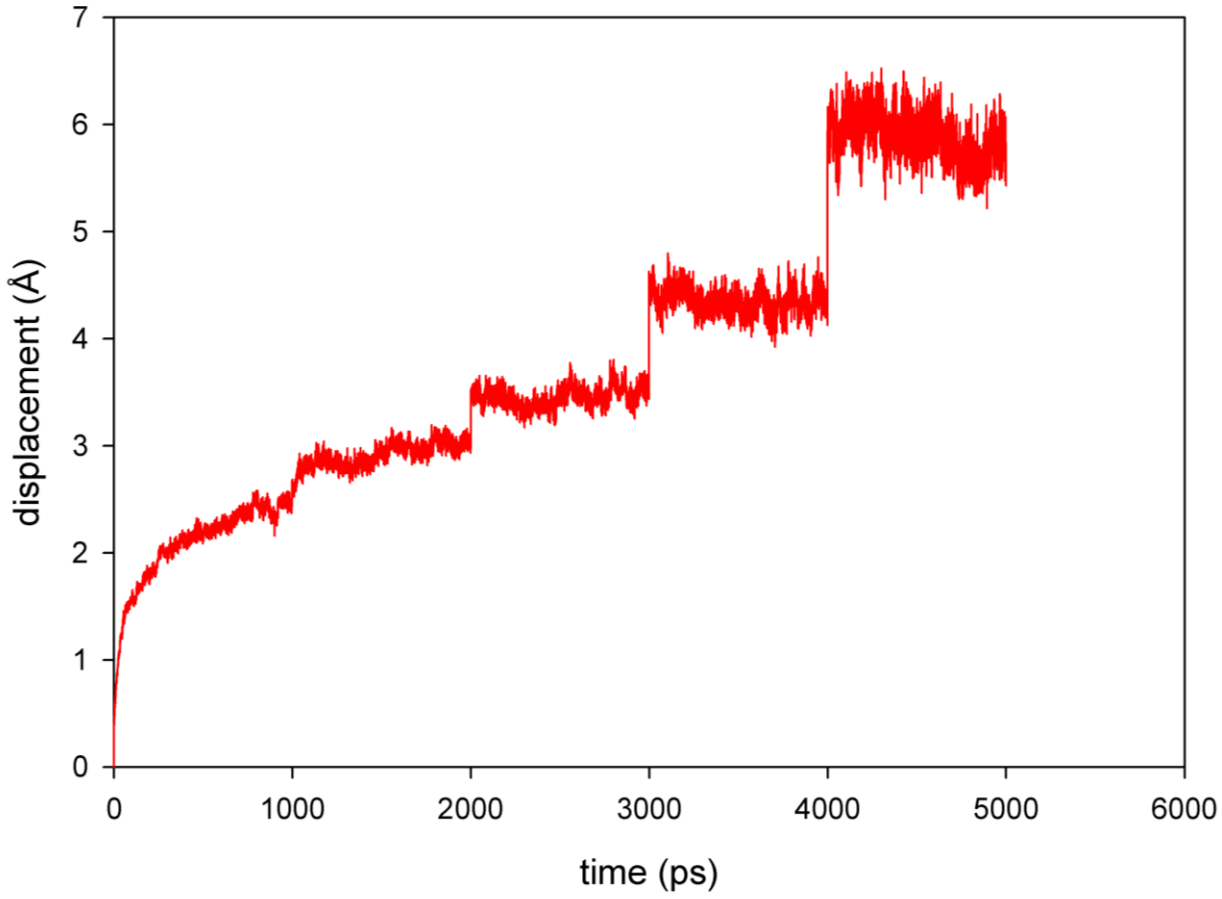

Figure 9, The variation of the displacement with time for a D5 penetrant at 300K using Dreiding *force field*

4.2.2 Effect of temperature on displacement

At higher temperatures, the penetrant trajectory is considerably different. Figure 10 shows the diffusion mechanism of D4 penetrant at 350K using Dreiding force field. There is no significant difference between figure 8 (300K) and figure 10 (350K). The residence time seems more or less the same in both figures, but in figure 10, from 3000ps to 5000ps, the residence time has doubled compared that in figure 8. This can be attributed to the density not being evenly distributed in figure 10. It looks like from 3000ps, the penetrant entered a region of high density. The magnitude of the displacement looks the same for both figures, despite the difference in temperature. In figure 11 which shows the type of motion the D4 penetrant undertook at 400K, the step like motion is not clearly visible as it was at 300K (figure 8). There is a significant decrease in residence time compared to figure 8. The channels for diffusive jumps seem to occur more often than in figure 8. The magnitude of the displacement has also increased (double that in figure 8 and 10). This is believed to be due to the higher thermal fluctuations of the polymer due to higher temperature. It appears the residence time is approximately the same throughout the diffusion process. This is quite clear in figure 8, where residence time is about 0.5 ns and in figure 9 it is approximately 1ns. However in figure 10 the residence time from 3000ps to 5000ps is about 1ns which is more than double that before 3000ps. Also towards the end of the simulation the jump event seems too long compared to jump event at the beginning, and in the middle of the simulation as can be seen in figures 8, 9, 10 and 11. This might be attributed to statistical errors. The analysis of the penetrant trajectories demonstrates a variation in the diffusion process with respect to temperature. At low temperature (300K) such as in figure 8, the penetrant diffuse

entirely by the hop and jump mechanism, the penetrant spent a longer time in a cavity, exploring the cavity, and in a short space of time the penetrant jump from one cavity to another. Diffusion at lower temperatures therefore seems to be limited by the number of cavities available to the penetrant in a polymer matrix and their distribution. At higher temperatures the residence time decreases as can be seen in figure 11. This is because at higher temperatures, the polymer is more mobile. The penetrant is no longer trapped in cavities. Therefore the diffusion at higher temperatures seems to be limited by the mobility of the polymer matrix. The magnitude of the diffusion also seems to be affected. There seems to be an increase in the mobility with an increase in temperature. This can be clearly seen in figure 8 (300K) and figure 11 (400K), the magnitude of the displacement is higher in figure 11 than in figure 8.

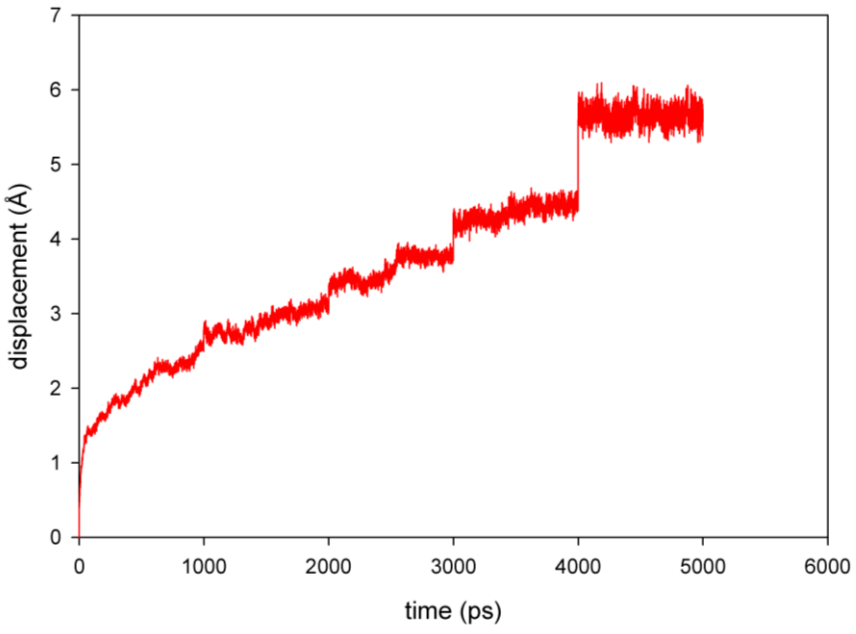

Figure 10, The variation of the displacement with time for a D4 penetrant at 350K using Dreiding *force field*

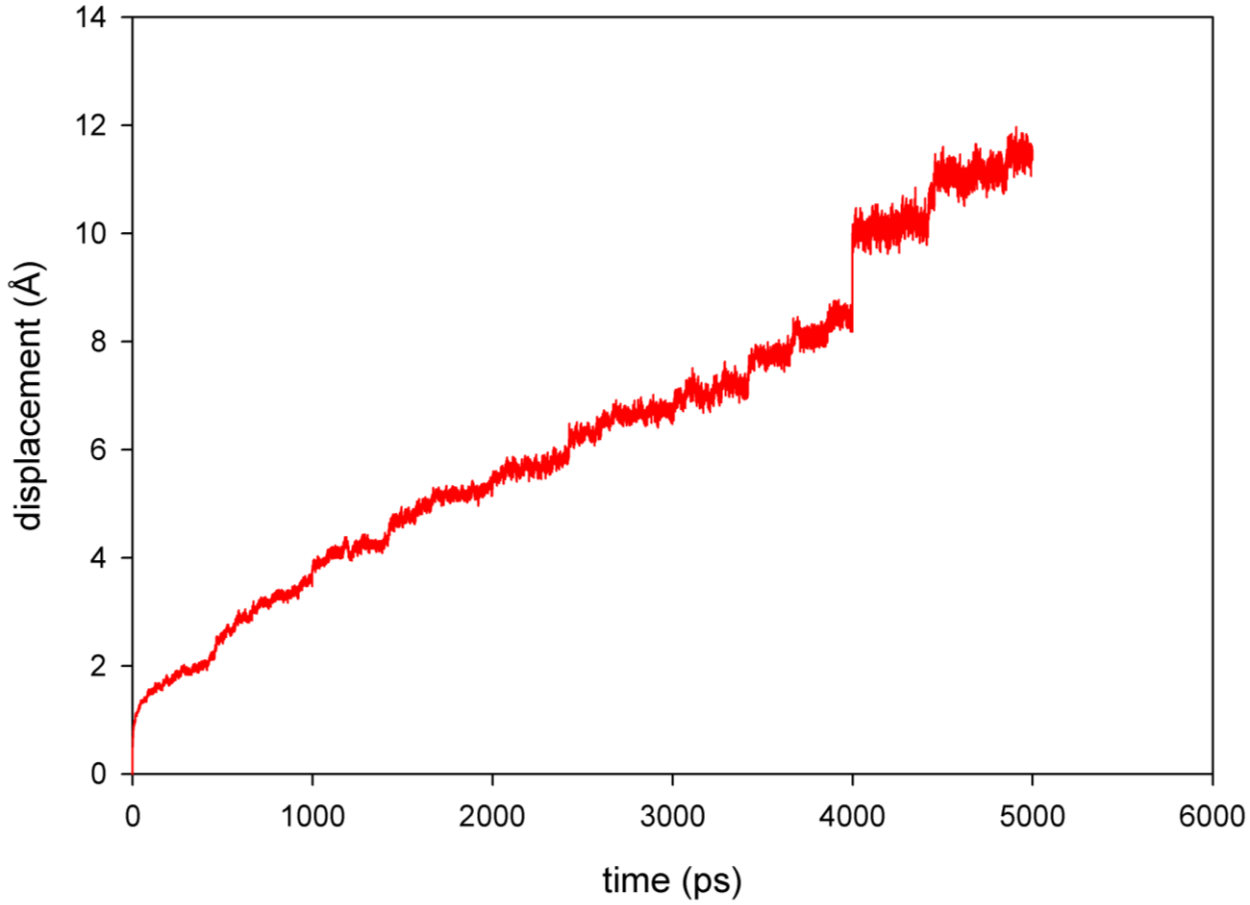

Figure 11, The variation of the displacement with time for a D4 penetrant at 400K using Dreiding *force field*

4.2.3 Mean squared displacement analysis

From the displacement graphs the mean square displacement of a molecule averaged over all simulated diffusing molecules can be calculated. It does not contain a more or less extended linear portion and has a noisy part at longer times. The non-linear portion of the curve is caused by statistical problems. From the linear part, the diffusion constant (D) is calculated using the Einstein equation. This equation relies on the assumption of a random walk for each penetrant through the polymer matrix. That means that the jump of a molecule between individual cavities determines the mean square displacement behaviour. The still rather short possible duration of MD simulation does, however, sometimes result in a non-negligible influence of very fast movement of permeate molecules inside the individual cavities. This in cavity motion is determined by the shape of the cavity and is therefore no random walk; is called anomalous diffusion that was first reported by Muller- Plathe [39]. The usual effect of anomalous diffusion is to create a somewhat smaller slope of the mean square displacement at lower time values. The type of diffusion taking place can be determined by the log (MSD) vs log (time) plot, as discussed in chapter 3.

Figure 12 shows the MSD vs time graph of D3 penetrant at 300K using Dreiding force field with the straight line starting from zero indicating the region on the graph where diffusion satisfies Einstein diffusion. The graph shows two types of diffusion, from the beginning to approximately 2800ps the motion was purely anomalous and from 2800ps to approximately 3700ps the graph shows real diffusive motion. This is indicated by figure 13 (the plot of log (MSD) vs log (time) graph) with the slope of less than unity for anomalous diffusion, and the slope of unity for real diffusion as

discussed in section 3.7. After 3700ps the diffusion deviate from normal diffusion, which is mainly due to statistical errors

Figure 14 shows the MSD vs time graph of D4 penetrant at 300K using Dreiding force field, with the straight line representing the region where normal diffusion took place. The graph shows two regions of linearity. The first region which is from approximately 500ps to 3500ps shows that the diffusion was purely anomalous. This was followed by a super diffusive motion [39, 62-66] which is linear from approximately 4200ps. The interval at which the straight line touches the graph or where random walk seems to be achieved is not linear. This can only be taken as a transition from anomalous diffusion to super diffusion. The same behaviour is seen in figure 15 which shows the MSD vs time graph of D5 penetrant at 300K using Dreiding force field, with the straight line representing the region where Einstein diffusion took place. For the most part of the simulation, the motion of D5 penetrant was purely anomalous from approximately 200ps to 3500ps and after that it was followed by super diffusive motion.

One might notice that for the smallest penetrant (D3), figure 12, the normal diffusion was reached at longer times, whereas for larger penetrants D4 and D5 the simulation time was not enough for normal diffusion to take place.

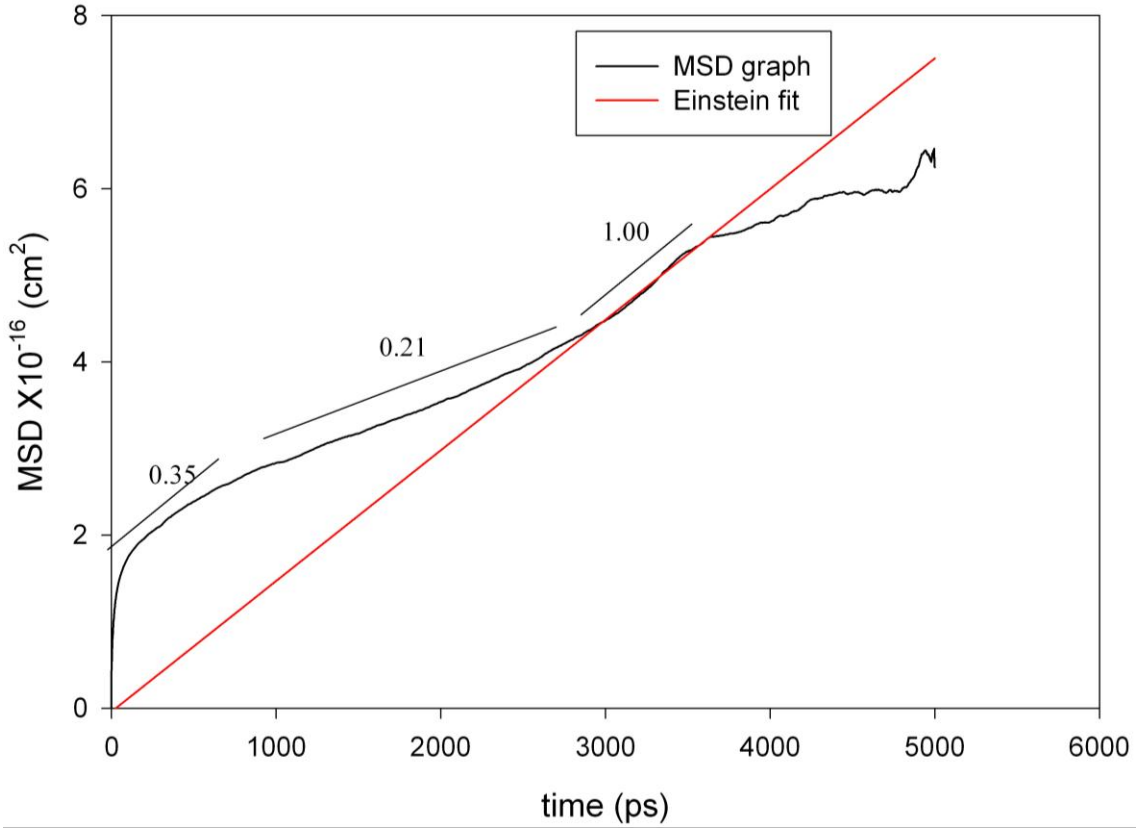

Figure 12, the MSD of D3 penetrant at 300K using Dreiding *force field, with the straight line starting from zero showing the region where Einstein diffusion took place. The short straight lines 0.35 and 0.21 showing the region where anomalous diffusion took place, based on the log MSD vs log time graph*

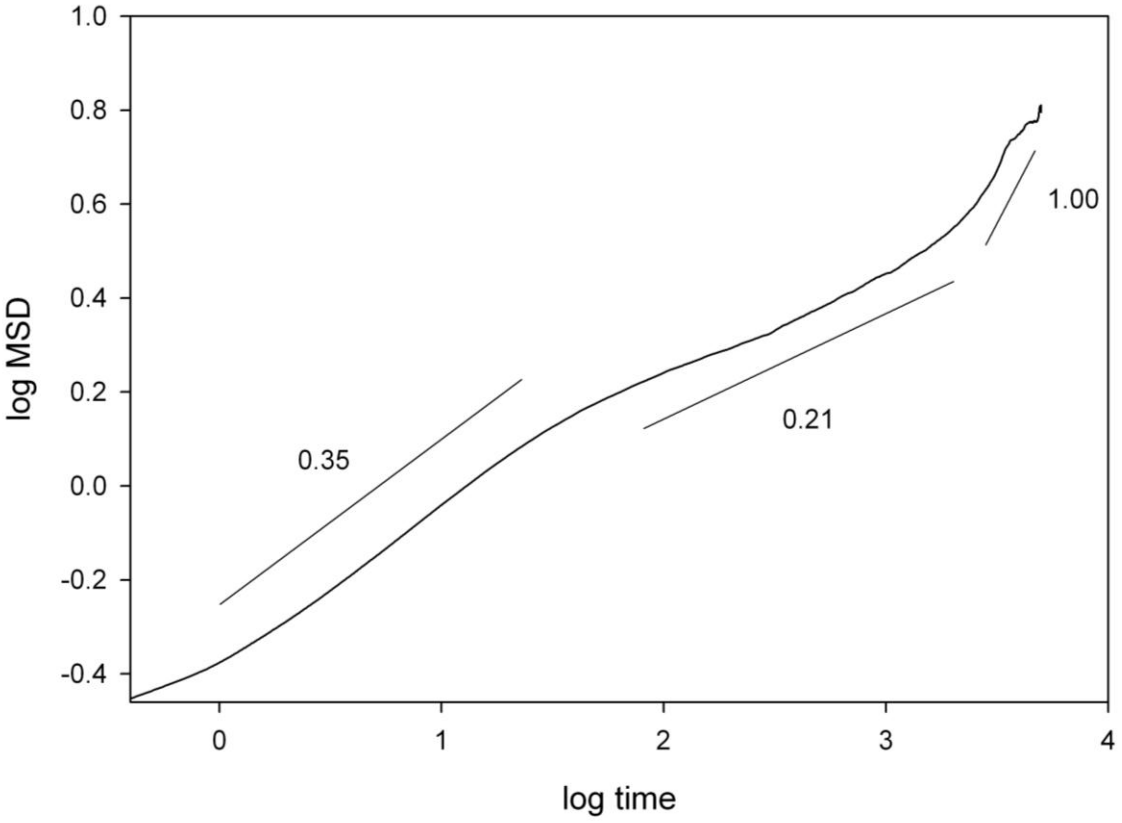

Figure 13 shows the log MSD vs log time graph of D3 penetrant using Dreiding *force field, with the straight line, 0.35 and 0.21 showing anomalous diffusion and, 1.00 showing where Einstein diffusion took place.*

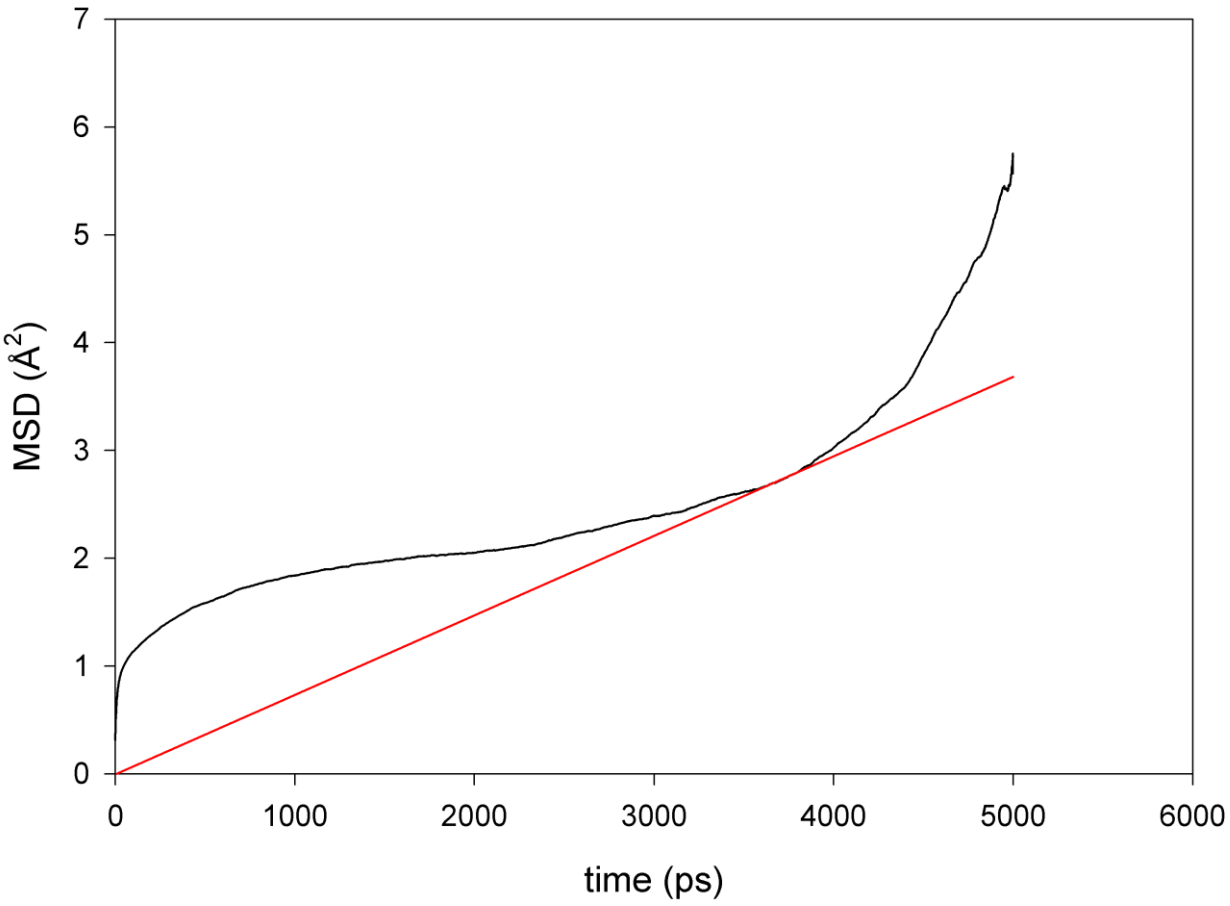

Figure 14 the MSD of D4 penetrant at 300K using Dreiding *force field, with the straight line representing the region where Einstein diffusion took place.*

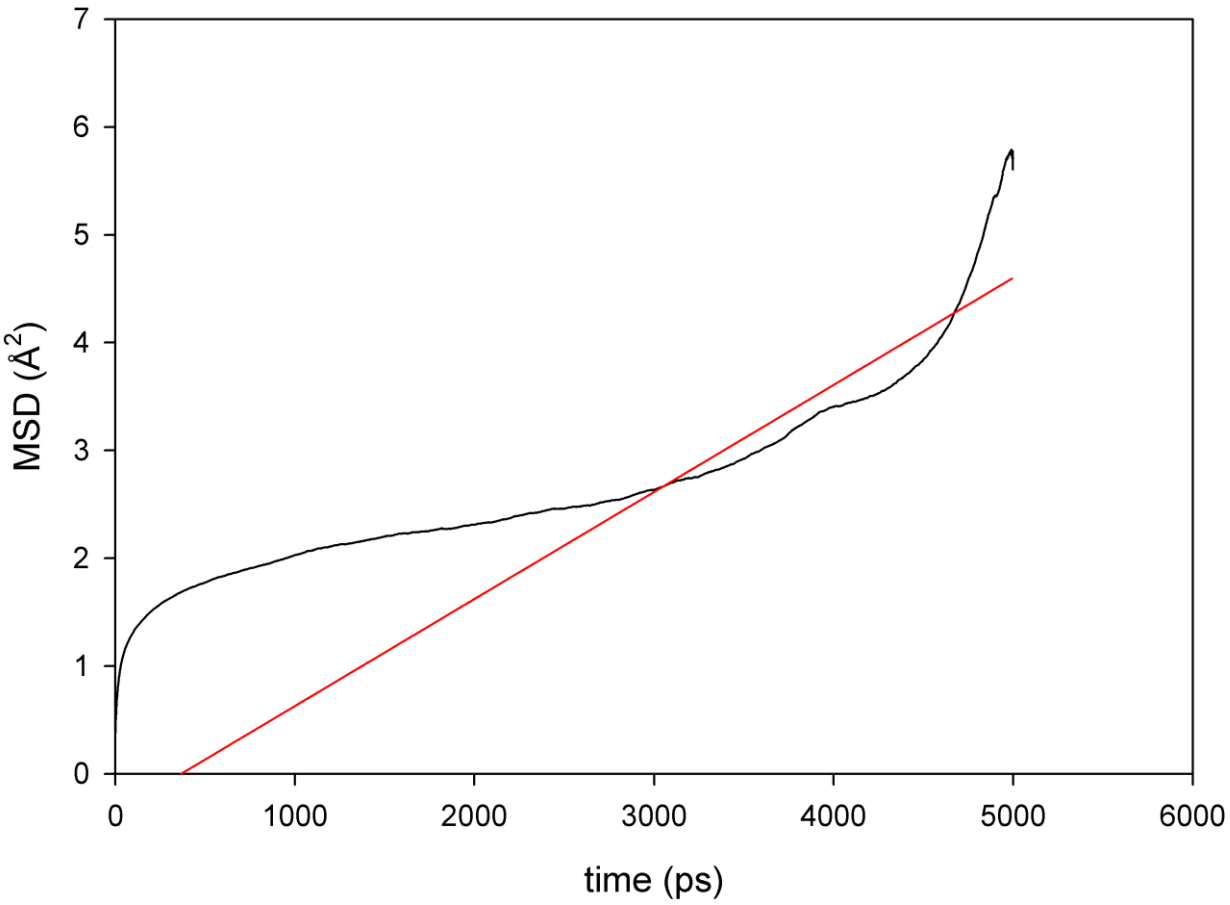

Figure 15 the MSD of D5 penetrant at 300K using Dreiding force field, with the straight line representing the region where Einstein diffusion took place.

Figures 16, 17 and 18 show the MSD vs time graphs of D3, D4 and D5 penetrants obtained using COMPASS force field at 300K respectively. All the graphs show anomalous diffusion prevailing throughout the simulation time. This is believed to be as a result of the outward projected hydrogen atoms that inhibit the diffusion of the penetrant as compared to the united atom approach used in Dreiding force field. It takes more time for normal diffusion to prevail for COMPASS force field simulations than for Dreiding force field as COMPASS force field uses the all atom approach. This is validated in figure 12 (D3 penetrant using Dreiding force field), where normal diffusion was achieved at longer times approximately 2800ps to 3700ps, whereas in figure16 (D3 using COMPASS force field), normal diffusion was never achieved for the same simulation time.

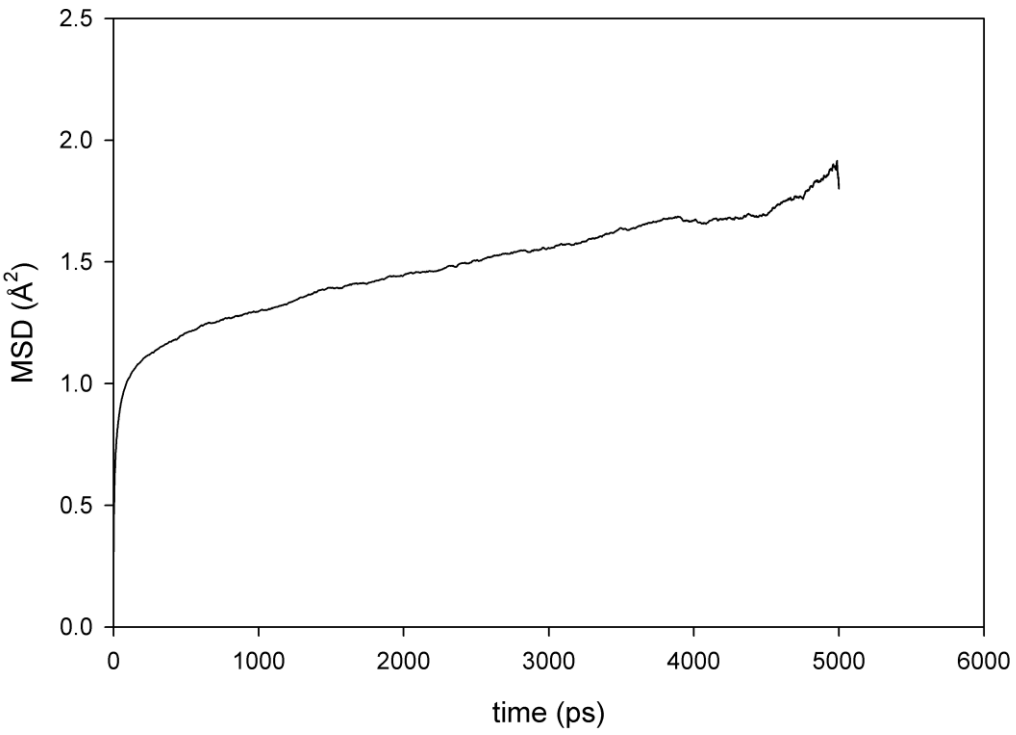

Figure 16 MSD graph of D3 penetrant at 300K using COMPASS *force field*

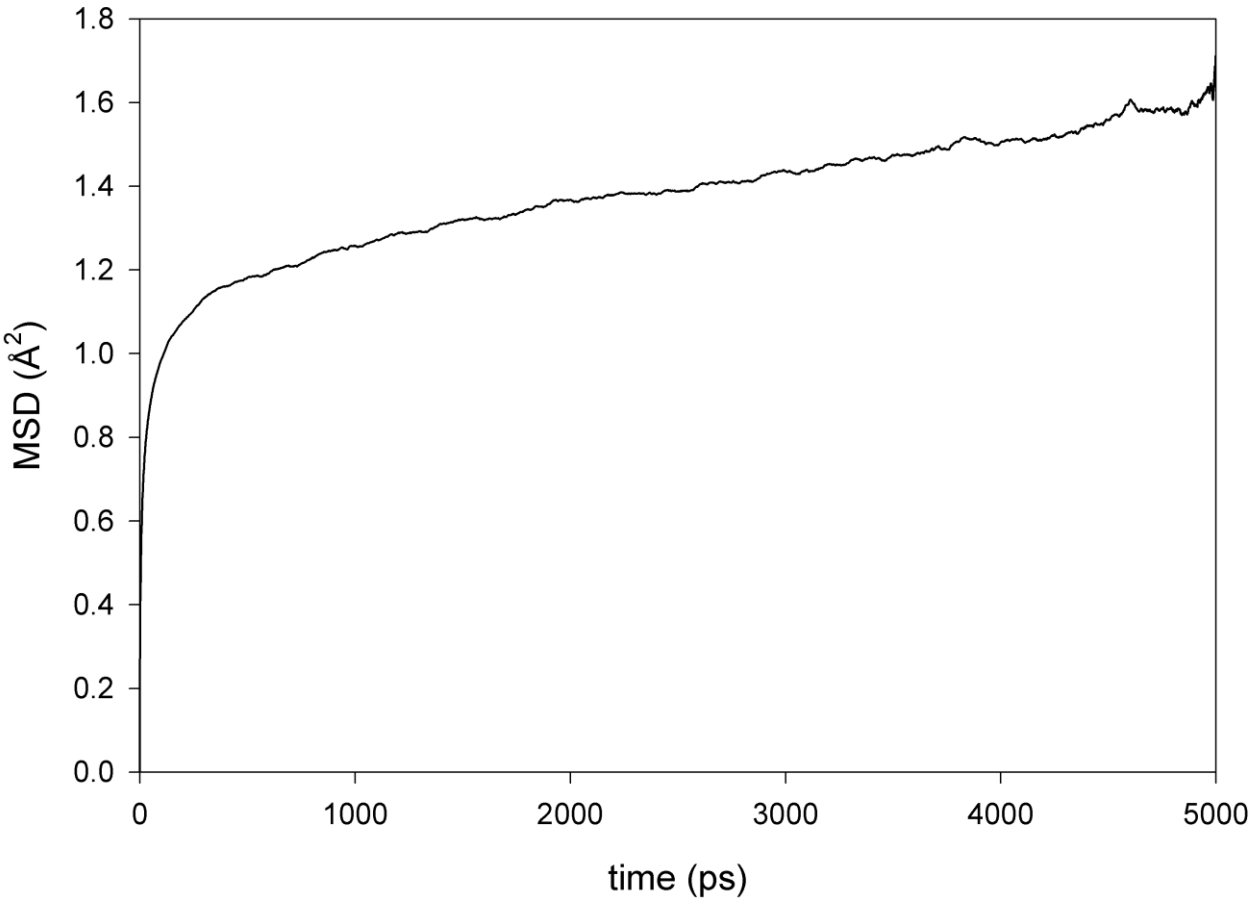

Figure 17 MSD graph of D4 penetrant at 300K using COMPASS *force field*

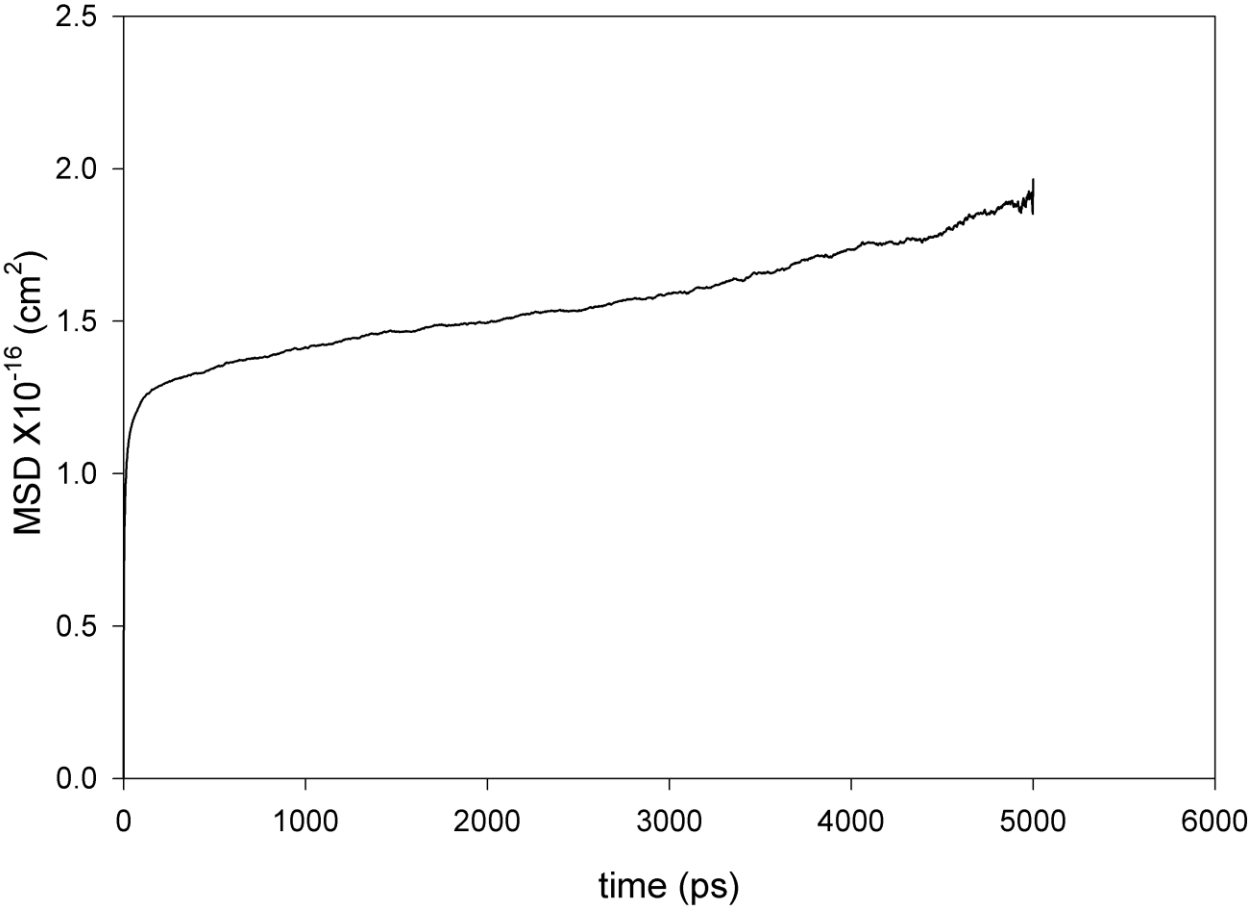

Figure 18 MSD graph of D5 penetrant at 300K using COMPASS *force field*

4.2.4 Calculated diffusion coefficients

The average diffusion coefficient in table 1 were taken over the entire simulation time, whereas the Einstein diffusion coefficients were taken in the interval where the log (MSD) vs log (time) graph gives the slope of unity and anomalous diffusion coefficient were taken from the linear part where it was found that the log (MSD) vs log (time) gives the slope of less than unity. Based on the discussion in section 4.2.2, the Einstein diffusion never occurred for all the systems for the entire simulation time except for D3 system. So the Einstein diffusion coefficients for D3 penetrant can be taken as the true diffusion coefficient, but for D4 and D5 penetrants the calculated diffusion coefficient are just the rough estimation of the real diffusion coefficient since the interval where the log (MSD) vs log (time) gives the slope of unity is not linear. The anomalous diffusion coefficients for Dreiding force field were calculated in order to compare with those obtained using COMPASS force field. For D3 penetrant (figure 12) the linear part where anomalous diffusion took place gives diffusion which is one order of magnitude higher than when using COMPASS force field (figure 16).

For D4 and D5 penetrant the diffusion coefficient is of the same order of magnitude for both COMPASS and Dreiding force field, but the magnitudes calculated using Dreiding force field are higher than those obtained using COMPASS force field as noted in table 1. This is due to the united atom approximation used in Dreiding force field as compared to the all atom approximation employed in COMPASS force field. The diffusion coefficient (anomalous) seems to fluctuate with increasing penetrant size as shown in table 1. The diffusion coefficient (anomalous) for both Dreiding and COMPASS force field follow the same trend (D3>D5>D4), contrary to the expected

trend of D3>D4>D5 as smaller penetrant are expected to diffuse faster than larger penetrants.

In table 2 an increase in temperature seems to increase the rate of diffusion of penetrants through the polymer. This is caused by the increase in mobility of the polymer at higher temperatures. The order of magnitude for D5 penetrant is the same as the one obtained by Hillborg et al who found the diffusion coefficient of D5 penetrant to vary from 1-20 x $10^{-8}$$cm^2.s^{-1}$ depending on the extraction depth [67].

Diffusion coefficients (x 10^{-8} cm^2/s) at 300K				
Silicone oils 20 Penetrant	Dreiding			COMPASS
	Average	Einstein	Anomalous	Anomalous
D3	1.551	2.515	1.190	0.234
D4	0.972	1.229	0.556	0.169
D5	0.962	1.655	0.641	0.196

Table 1, Diffusion coefficients of cyclic PDMS oligomers in PDMS polymer, with the average being taken from the entire simulation time, Einstein diffusion coefficient taken where the slope satisfies Einstein equation and Anomalous taken from the linear part of the graph. The simulation time was 5000ps.

D4	Diffusion coefficient (D) x 10^{-8} cm^2/s
300	1.229
350	1.748
400	3.918

Table 2, Diffusion coefficient coefficients of D4 penetrant in PDMS polymer, with the Einstein diffusion coefficient taken where the slope satisfies Einstein equation

As discussed in section 4.2.2 a change in temperature will affect both the penetrant and the polymer dynamics. The penetrant will have an increased energy and so will be able to jump to cavities that are blocked by higher energy barriers. The temperature effect on the polymer is to increase the segmental motion, which results in the redistribution of the cavities. This redistribution of cavities often results in inter-connection of cavities, and if a penetrant has enough energy to overcome the potential barrier it will jump to the next cavity. This temperature dependency of a diffusion process can be determined by the Arrhenius equation of the form

$$D = D^* e^{-\frac{E_a}{RT}} \tag{37}$$

where D^* is the pre-exponential factor, R is the gas constant, E_a is the activation energy, that is the energy a diffusing particle must posses for a successful jump from one cavity to another. Taking the natural logarithm of the Arrhenius equation yields

$$\ln D = \ln D^* - \frac{E_a}{R}\frac{1}{T} \tag{38}$$

For a process to obey Arrhenius equation, a plot of $\ln D$ versus $\frac{1}{T}$, must give a straight line, whose slope and intercept can be used to determine E_a and D^*. E_a was calculated and found to be 11.27KJ/mol. Not enough data was sampled to accurately predict unambiguously the values of the activation energy (E_a), as can be seen from the Arrhenius plot. More points must be plotted for the graph to clearly show whether Arrhenius behaviour was obeyed or not.

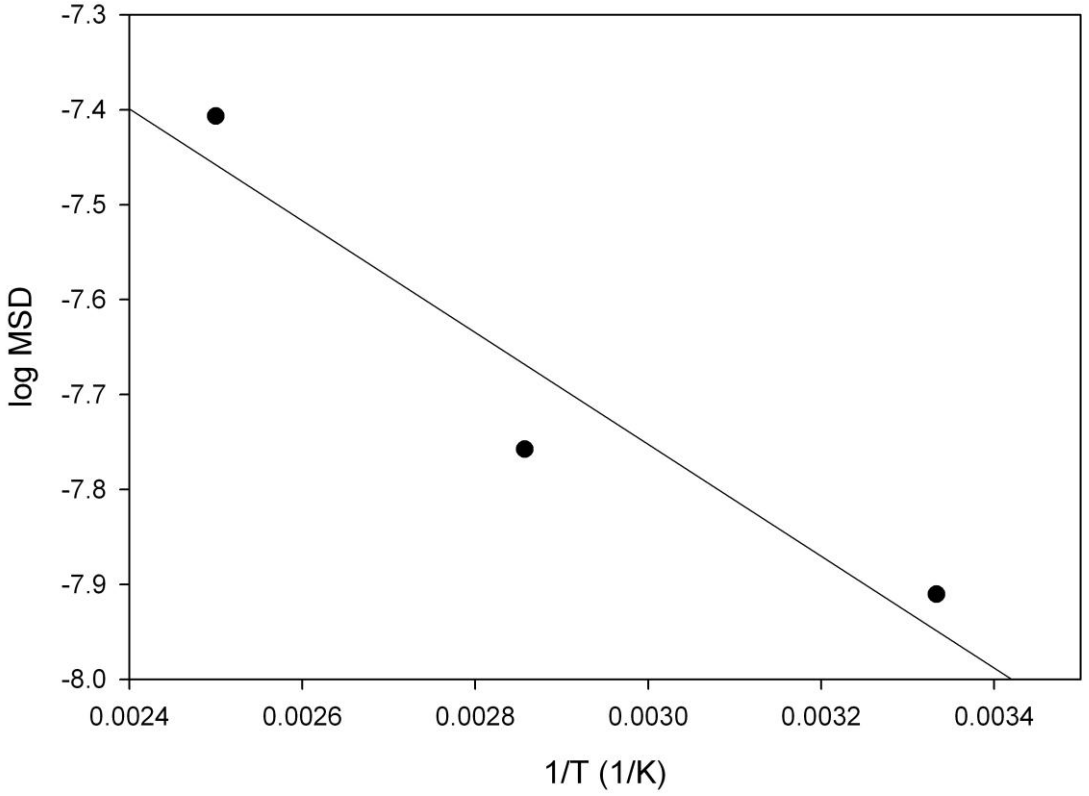

Figure 19 the Arrhenius plot of log Diffusion coefficient versus inverse Temperature for D4 penetrant using Dreiding *force field*

4.3 Validation

DMol3 is a unique, accurate and reliable density functional theory (DFT) quantum mechanical code for research in the chemicals and pharmaceutical industries. It combines computational speed with the accuracy of quantum mechanical methods to predict materials properties both reliably and quickly. It is highly versatile and can be applied to research problems in the gas phase, solvent solid state, in chemistry, materials science, chemical engineering, and solid state physics.

The density functional theory methods are based on a variety of functionals. The first of these is the local density approximation (LDA), for which the exchange-correlation functional consists of the Dirac-Slater exchange and the Vosko, Wilks and Nadir (VWN) correlation terms. Note that the correlation term is the VWN fitting of the electron gas simulations of Ceperlay and Alder and not the VWN RPA result, which is an approximation to the correlation energy. The other functionals are all 'gradient corrected' (sometimes called non-local) functionals (GGA). The the first of these functionals, denoted BLYP, is obtained by adding gradient corrections to the LDA method - specifically the exchange correction of Becke and the correlation function of Lee, Yang and Parr. The BLYP functional has been widely used in theoretical chemistry. Further information about DFT can be found in the references [68-73]

Calculation of structural properties was performed on silicone oil (cyclic PDMS oligomers) to determine which of the two force field best describe our system. The results obtained from calculations using COMPASS and Dreiding force field were compared with those obtained from Dmol calculation which uses Density Functional Theory (DFT).

Polysiloxane are extremely flexible molecules due to the free rotation about the Si-O and the Si-C bond with PDMS exhibiting the most flexibility. The Si-O-Si bond angle for a linear chain has been shown to vary as a function of measurement technique [75] as can be seen in table 3. A generally accepted value for the Si-O-Si bond angle is 143° and C-Si-C bond angle is 111° [75].

Bond Angles	Gromos FF[48]	PCFF[61]
Si-O-Si	144	157
O-Si-O	109.5	110.7
O-Si-C	109.5	114.9
C-Si-C	109.5	114.9
Si-C-H		111.5

Table 3, shows the bond angles of a PDMS linear chain

In table 4, 5 and 6, the bond angles and bond length are shown. The values obtained in all the tables seem to be in good agreement except for the Si-O-Si angle when using Dreiding force field in all the tables. Dreiding force field seems to underestimate the Si-O-Si angle.

In table 4 which shows the bond angles of D3 penetrant, the Si-O-Si bond angles values are low as compared to Table 3, 5 and 6. The Si-O-Si bond angles in table 4 for a D3 penetrant are very low as compared to those in table 3 (for a linear chain). This is in agreement with what Mechan [75] found. This is an indication that the D3 molecule is highly strained. Furthermore Flory et al [74] found that the O-Si-O is some what low (104°) compared to the typical O-Si-O bond angle. COMPASS force

field seems to confirm his findings, with the other generating a slightly higher angle. This further confirms that the D3 molecule is strained, hence unstable. In table 5 and 6 the bond angles compare reasonably with those of a linear chain. The bond length in all the penetrants D3, D4 and D5 seems not to be affected by the size of the penetrant. They all compare reasonably with those of the linear chain. Although Dreiding force field seems to underestimate the bond length.

It looks like Dreiding force field somehow generate a smaller molecule due to shorter bond angles and bond length which might the reason why the MSD obtained using Dreiding force field shows region of normal diffusion in our simulation whereas for COMPASS force field there is no region where normal diffusion took place.

Bond Angles (°)						
	COMPASS[a]	COMPASS[b]	Dreiding	Dmol		exp
				LDA	GGA	
Si-O-Si	131.901	131.901	114.866	132.624	132.519	136 [74,75]
O-Si-O	105.076	105.076	113.974	107.344	107.480	104 [74,75]
O-Si-C	109.610	109.610	108.605	109.254	109.335	
C-Si-C	113.010	113.010	108.132	112.354	111.890	
Si-C-H	111.432	111.432	109.880	110.934	111.026	
H-C-H	107.441	107.441	109.059	108.080	107.845	

(a)

Bond Length b_0 (Å)					
	COMPASS [a]	COMPASS[b]	Dreiding	Dmol	
				LDA	GGA
Si-O	1.644	1.644	1.604	1.649	1.666
Si-C	1.886	1.886	1.705	1.844	1.867
C-H	1.100	1.100	1.090	1.103	1.099
O-O	2.610	2.610	2.690	2.657	2.687
Si-Si	3.003	3.003	2.704	3.020	3.050

(b)

Table 4 (a) and (b) The bond angle and bond length of D3 penetrant respectively

Bond Angles (°)					
	COMPASS[a]	COMPASS[b]	Dreiding	DMol	
				LDA	GGA
Si-O-Si	145.712	145.569	122.292	139.462	148.729
O-Si-O	107.627	107.630	113.146	109.529	110.140
O-Si-C	109.380	109.296	109.120	108.545	108.610
C-Si-C	111.848	111.927	105.943	113.096	112.234
Si-C-H	111.699	111.422	110.035	110.982	111.085
H-C-H	107.364	107.452	108.900	107.918	107.810

(a)

Bond Length (Å)					
	COMPASS[a]	COMPASS[b]	Dreiding	DMol	
				LDA	GGA
Si-O	1.634	1.634	1.605	1.642	1.654
Si-C	1.888	1.888	1.708	1.846	1.869
C-H	1.101	1.100	1.090	1.103	1.099
O-O	1.638	2.638	2.676	2.673	2.714
Si-Si	3.123	3.122	2.812	3.082	3.186

(b)

Table 5 (a) and (b) The bond angle and bond length of D4 penetrant respectively

Bond Angles (°)					
	COMPASS[a]	COMPASS[b]	Dreiding	DMol	
				LDA	GGA
Si-O-Si	149.480	144.919	123.903	138.894	148.318
O-Si-O	108.042	107.285	108.795	108.890	109.112
O-Si-C	109.335	109.099	110.017	108.585	108.860
C-Si-C	111.388	112.280	107.279	113.519	112.221
Si-C-H	111.474	111.401	110.107	110.915	111.082
H-C-H	107.395	107.463	108.711	107.998	107.812

(a)

Bond length (Å)					
	COMPASS[a]	COMPASS[b]	Dreiding	DMol	
				LDA	GGA
Si-O	1.632	1.634	1.610	1.644	1.653
Si-C	1.889	1.887	1.708	1.844	1.870
C-H	1.101	1.100	1.089	1.103	1.099
O-O	2.641	2.632	2.613	2.675	2.693
Si-Si	3.144	3.113	2.841	3.077	3.177

(b)

Table 6 (a) and (b) The bond angle and bond length of D5 penetrant respectively

[a] Materials Studio calculations using Discover code

[b] Cerius2 calculations using Off-methods code

4.4 Limitations of molecular dynamics

MD is a computationaly intensive procedure [76] with simulations of several nanoseconds taking a few months in cpu time on a modern workstation. In these simulations it took two months for Dreiding force field simulations of 5ns and almost

3 months when using COMPASS force field for the same simulation time. Some of the factors that cause MD to be so intensive are the size of the system, rate of diffusion of the penetrant through the polymer, and force field used.

The polymer simulated must be large enough to ensure distribution of free volume and polymer configurations that reasonably match those found in reality. Even with quite small monomer unit this can often mean thousands of atoms being used.

To obtain real values of diffusion coefficient, it is necessary to sample a sufficient number of jump events during simulation. With a small penetrant in a relatively permeable polymer this is easily achieved within few hundreds pico seconds of simulation. But as the size of the penetrant increases as is the case in our simulation (all the penetrants used, D3, D4 and D5 are large), the number of jump events decreases significantly and so to sample sufficient number of jumps for accurate diffusion coefficient calculation the simulation must be run for a long time.

When using force fields that uses a united atom approach, the number of interactions in the polymer and penetrant are reduced and it turns to speed up the rate of simulation, however for all atom force fields, all interactions are calculated including the hydrogen interactions and furthermore, the outwards projected atoms turn to form obstacles in the jump events and hence reduces the number of jump sufficient for accurate prediction of diffusion coefficient. This will lead to longer simulation time needed for sufficient jumps for accurate prediction of diffusion coefficient and it will take more time to compute all interactions. This is indicated by the shorter time spent to simulate a D3 penetrant system using Dreiding force field (which uses a united

atom approach) to reach the long time limit than that of COMPASS force field (which uses an all atom approach).

CHAPTER 5

CONCLUSION AND RECOMMENDATIONS

Conclusions are drawn based on the results and discussion and recommendations will be made**.**

5.1 Conclusion

Diffusion of PDMS oligomer in PDMS polymer matrix has been studied using molecular dynamics. The study has brought about useful information on how diffusion in PDMS is influenced by penetrant size, temperature and force fields. Molecular dynamics has confirmed, from penetrant displacement against time curves, that diffusion of PDMS oligomer through PDMS polymer matrix occurs by hop and jump mechanism with the permeates spending long periods of time trapped within one void and occasionally jumping between voids. It has been further noted that the jumps 1longer time in one cavity than smaller penetrants and hence diffuse slower than smaller penetrant. This further confirms that the jump event determines the diffusion in polymer, not the motion of a penetrant in a cavity. An increase in temperature results in an increase in diffusion coefficient. This allows increased mobility of PDMS oligomers which will result in faster recovery of PDMS based insulators.

The magnitude of diffusion coefficient using Dreiding force field for D5 is of the same order of magnitude as the experimental values [67]. The results of Dreiding force field are generally higher than those of COMPASS force field. This might be ascribed to the united atom approach used in Dreiding force field as discussed in section 4.3, it generated a somewhat smaller penetrant compared to COMPASS force

field. Generally, owing to the united atom approach, Dreiding force field is expected to produce diffusion coefficients which are slightly higher compared to COMPASS force field which uses an all atom approach. Furthermore when using COMPASS force field much longer simulation time is needed as compared with Dreiding force field which is as a result of the united atom approximation applied in Dreiding force field. However from the tables of bond length and bond angles, COMPASS force field seems to describe our system better.

Molecular dynamics is a useful tool for studying diffusion of small molecules, but for larger molecules the time scale is not long enough for molecules to reach the long time limit for normal diffusion to take place. It needs to be developed, to be able to simulate well in to the ms region or more. However from the results generated, MD managed to predict how the large penetrants move in a polymer matrix.

5.2 Recommendations

Extensive research need to be done on experimental work on the diffusion of PDMS oligomers at various temperatures. There is a need to study types of filler that can strengthen the material and not impede too much on the diffusion of low molecular weights to the surface.

5.3 Reference

[1] http://www.utilityproducts.com/Articles/2005/08/returnclarity.htm**,** Insulators of toughened glass for HV lines are again earning praise and popularity, by Joe Renowden and Ezio Del Bello,

[2] R. S. Gorur, E. A. Cherney, J. T. Burnham, Outdoor Insulators, Ravi S. Gorur Inc, Phoenix, Arizona 85044 USA, (1999)

[3]http://www.elkraft.chlmers.se/Publikationer/HSP.pub/Abstract/2000/gustavssonLic/chap1_2.pdf

[4] Kleberg insulator pollution test station (kipts) from research facility to an in house insulator product ageing test standard by W. L. Vosloo, R. Swinny and T. Mvayo.

[5] M. W. Skinner, C. Qian, S. Grigoras, D. J. Halloran, and B. L. Zimmerman, Textile Res. J. 69, 935, (1999)

[6] J. Kim, M. K. Chaudhury and M. J. Owen, IEEE trans. on Dielectric and electrical insulation, vol.6 no.5 October 1999

[7] Polymer Solutions to contaminated environments by Steve Brewer Ohio Brass, presented to the southeastern electrical exchange 13/09/1994B

[8] S. H. Kim, E.A. Cherney, R. Hacham, K. G. Rutherford, IEEE Transactions DEI, 1, 106, (1994)

[9] R.S. Gorur, E. A. Cherney, R. Hackam and T. Orbeck, IEEE Transactions PD, 3, 1157, (1988)

[10] J. Kindersberg, A. Scutz, H. C. Karner, R.V.D. Huir, Service Performance, Material Design and Applications of Composite Insulators With Silicone Rubber Housings, CIGRE Session Paper, 33-303, p. 1-5, (1996)

[11] R. R. Maphanga, Computational Modelling and EXAFS studies of electrolytic Manganese Dioxide, PhD Thesis-2005, University of Limpopo

[12] B. J. Alder and T. E. Wainwright, J. Chem. Phys. 27, 1208, (1957)

[13] B. J. Alder and T. E. Wainwright, J. Chem. Phys. 31, 459, (1959)

[14] A. A. Gusev and U. W. Suter, J. Chem. Phys., 99, 2228, (1993).

[15] A. A Gusev, S. Arizzi, U. W. Suter and D. J. Moll, J. Chem. Phys., 99, 2221, (1993).

[16] A. A. Gusev, F. Müller-Plathe, W. F. van Gusteren and U. W. Suter, Adv. Polym. Sci., 116, 207, (1994).

[17] A. A Gusev, U. W. Suter and D. J. Moll, Macromolecules, 28, 2582, (1995).

[18] R.A Reis, J. Vladimir` Oliveira and R. Nobrega, Braz. J. Chem. Eng., 18, 367, (2001).

[19] Lydia Fritz and D. Hofmann, Polymer, 38, 1035, (1997).

[20] Dissertation by D. J. Van der Wal, Improving the properties of polymer blends by reactive compound, University of Groningen**,** (1998).

[21] H Homma, C. L. Mirley, J. Ronzello and S. A. Boggs, IEEE Trans. on Power Delivery, 15, 1298, (2000).

[22] E. D. Lykissa, S. V. Kala, J. B. Hurley and R. M. Lebovitz, Anal. Chem., 69, 4912, (1997).

[23] I De Bo, H. van Langenhove, P. Pruuost, J. De Neve, J. Pieters, I. F. J. Vankelecom and E. Dick, J. Mem. Sci., 215, 303, (2003).

[24] S. Grigorias, T. H. Lane, "comfomational Analysis of substituted polysiloxane polymers" in "Silicon-based polymer science"ed. By J. M. Zeigler and F. W. Fearon ISBNO-8412-1546, (1990).

[25] J. Kim, M. K. Chaudhury, M. J. Owen, IEEE Trans. Dielectrics EI, 6, 695, (1999).

[26] A. Colas and J. Curtis, Silicone Biomaterials: History and chemistry and medical applications of silicone, Dow corning Corporation, reprinted from Biomaterials Science, 2nd Edition, (2005).

[27] F. O. Stark, J. R. Falenda and A. P. Wright, Silicones in Comprehensive Organometallic Chemistry, Vol. 2, (1982)

[28] J. M. Zielinski and J. L Duda, AIChE Journal, 38, 3, (1992).

[29] S. J. Clarson, J. A. Semlyn, Siloxane Polymer Englewood Cliffs, NJ, Prentice Hall, (1993).

[30] J. E. Mark, H. R. Allock, R. West, Inorganic Polymers Englewood Cliffs, NJ, Prentice Hall, (1992).

[31] W. Noll, The Chemistry and technology of silicones, New York, Academic Press, (1968).

[32] H. Hillborg and U. W. Gedde, Polymer, 39, 1991, (1998).

[33] M. J. Owen and P. J. Smith, J. Adhesion Sci. Technology, 8, 1063, (1994).

[34] A. Toth, I. Bertoti, M Blazso, G. Banhegyi, A. Bognar and X. Szaplonczay, J. Appl. Polym. Sci., 52, 1293, (1994).

[35] M. J. Owen, Australian J. of Chem., 58, 433, (2005).

[36] H. Sun, J. Phys. Chem. B, 102, 7338, (1998).

[37] S. L. Mayo, B. D. Olafson and W. A. Goddard III, J. Phys. Chem., 94, 8897, (1990).

[38] R. S. Roe (Ed) Computer simulation of polymer. Prentice Hall, Englewood Cliff, NJ, (1991).

[39] F. Müller -Plathe, J. Chem. Phys., 96, 3200, (1992).

[40] J. I. McKechni, D. Brown and J. H. R. Clarke, Macromolecules, 25, 1562, (1992).

[41] D. Brown, J. H. R. Clarke, M. Okuda and T. Yamazaki, J. Chem. Phys., 100, 6011, (1994).

[42] P. J. Flory, Principles of Polymer Chemistry, Cornell University Press, New York, (1953)

[43] D. N. Theodorou and U. W. Sutter, Macromolecules, 18, 1467, (1985).

[44] R. Khare, M. E. Paulaitis and S. R. Lustig, Macromolecules, 26, 7203, (1993).

[45] M. Kotelyanskii, N. J. Wagner and M. E. Paulaitis, Macromolecules, 29, 8497, (1996).

[46] J. Bicerano and D. J. Moll, Computational and Theoretical Polymer Science, 6, 117, (1996).

[47] R. H. Boyd and P. V. K. Pant, Macromolecules, 24, 6325, (1991).

[48] R. M. Sok, Permeation of Small Molecules Across a Polymer Membrane: A Computer Simulation Study, Ph.D. Thesis, University of Groningen, (1994).

[49] J. R. M. Sok, H. J. C. Berendsen and W. F. van Gunstenren, J. Chem. Phys., 96, 4699, (1992).

[50] G. Couarraze URA CNRS 1218-University of Paris South 92296 Chatenay Malabry-France, Diffusion in polymers.

[51] S. Kashihara, M. Iotov, S. Dasgupta, G. Gao, M. Belmares, and W. A. Goddard III, Diffusion of Gases in Amorphous Polymers: The Monte Carlo Void Method Based on Molecular Dynamics; Application to He Diffusion in Polyethylene, Materials and Process Simulation Center, Beckman Institute (139-74), Division of Chemistry and Chemical Engineering, California Institute of Technology, Pasadena, California 91125, J. Chem. Phys. # 5016

[52] M. P. Tildesley, Computer Simulation of Liquids, Oxford University, Publishers, Oxford, (1987).

[53] F. Müller-Plathe, Acta Polymer, 45, 259, (1994).

[54] D. Hofmann, J. Ulbrich, D. Fritsch and D. Paul, Polymer, 37, 4773, (1996).

[55] D. Hofmann, L. Fritz, J. Ulbrich and D. Paul, Polymer, 38, 6145, (1997).

[56] F. Müller-Plathe, S. C. Rogers and W. F. van Gunsteren, J. Chem. Phys., 199, 237, (1992).

[57] F. Müller-Plathe, J. Membrane Science, 141, 147, (1998).

[58] V. M. Shah, S. A. Stern, P. J. Ludovice, Macromolecules, 22, 4660, (1989).

[59] D. Hofmann, L. Fritz, J. Ulbrich and D. Paul, Computational and Theoretical Polymer Science, 10, 419, (2000).

[60] F. Müller-Plathe, S.C. Rogers and W.F. van Gunsteren, Polymer Prep., Am. Chem. Soc., Div. Polym. Chem., 33, 633, (1992).

[61] L. Fritz and D Hofmann, Polymer, 38, 1035, (1997).

[62] I. M. Sokolov, J. Mai and A. Blumen, Phys. Rev. Lett., 79, 857, (1997).

[63] S. S. Manna, A. J. Guttmann, and B. D. Highes, Phys. Rev. B 39, (1989).

[64] D. Brockmann and T. Giesel, Phys. Rev. Lett., 91, 048303-1, (2003).

[65] A. Caspi, R. Granek and M. Elbaum, Phys. Rev. Lett., 85, 5655, (2000).

[66] A. van Oudenaarden and J. A. Theriot, Nature Cell Biology, 1, 493, (1999).

[67] H Hillborg, S. Karlsson and U. W. Gedde, Polymer, 42, 8883, (2001).

[68] P. Hohenberg and W. Kohn, Phys. Rev., 136, B864, (1964).

[69] W. Kohn and L. J. Sham, Phys. Rev. 140, A1133, (1965).

[70] R. O. Jones and O. Gunnarsson, Rev. Mod. Phys., 64, 689, (1989).

[71] B. G. Johnson, P. M. W. Gill and J. A. Pople. J. Chem. Phys., 98, 5612, (1993).

[72] E. Wimmer, Mathematical Methods for Digital Computer, J.K. Labanowski and J.W. Andzelm, ed. Spinger-Verlag: New York, p. 7. (1991)

[73] T. Zeigler. Chem. Rev., 91, 651, (1991).

[74] P. J. Flory; V. Crescensi and J. E. Mark, J. Am. Chem. Soc., 86, 146, (1964)

[75] Synthesis and characterization of cycloaliphatic and aromatic polymer/poly(dimethylsiloxane) segmented copolymer thesis by Jeffrey. Mechan (1997)

[76] Simulation of small molecule permeability in polymers, A Dissertation for the certificate of postgraduate study – June 1996 by Paul Hadgett

5.4 Appendix

5.4.1 Papers presented

1 T. Kubai*, J.J. Dolo*, P. E. Ngoepe and L. Ackermann, Transport properties, behaviour of penetrants in nafion membrane: A molecular dynamics simulation study. Presented at South African Institute of Physics (SAIP), University of Stellenbosch, June 2003

2 T. Kubai*, P. E. Ngoepe and L. Ackermann, Diffusion of polydimethylsiloxane (PDMS) in PDMS. Presented at Interscience conference, University of the North, October 2003

3 T. Kubai*, P. E. Ngoepe and L. Ackermann, Diffusion of polydimethylsiloxane (PDMS) membrane of insulators. Presented at Material Modelling Meeting, University of the North, March 2004

4 T. Kubai*, P. E. Ngoepe and L. Ackermann, Diffusion of polydimethylsiloxane (PDMS) membrane of insulators. Presented at South African Institute of Physics (SAIP), University of the Free State, June-July 2004

5 T. Kubai*, P. E. Ngoepe and L. Ackermann, Diffusion of polydimethylsiloxane (PDMS) membrane of insulators. Presented at Material Modelling Meeting, University of Limpopo, March 2005

6 T. Kubai*, P. E. Ngoepe and L. Ackermann. The study of Structural properties and diffusion of PDMS oligomers in PDMS matrix. Presented at South African Institute of Physics (SAIP), University of Pretoria, July 2005